Soft magnetic materials, from statics to radiofrequencies

Victorino Franco

Sevilla University. Spain

Current trends in Magnetic Refrigeration

- Magnetocaloric materials:
  - Giant magnetocaloric materials
  - Second order phase transition materials
  - Nanostructured materials
  - Multiphase materials and composites
- Modeling the magnetocaloric effect
- Experimental techniques for the characterization of magnetocaloric materials
- Magnetic refrigeration devices
- Related topics on thermomagnetic energy harvesting

Confirmed invited speakers

- J. I. Betancourt Reyes (UNAM);
- E.H. Bruck (Delft University of Technology);
- G.P. Carman (UCLA);
- A. Fujita (Tohoku University);
- Z.W. Liu (South China University of Technology);
- V.K. Pecharsky (Ames Laboratory);
- M.H. Phan (University of South Florida);
- A. Rowe (University of Victoria);
- J. L. Sánchez Llamazares (IPICYT);
- K. Skokov (Technische Universität Darmstadt);
- K. G. Suresh (IIT Bombay).

http://www.mrs.org/imrc-2013-cfp-7b/

Victorino Franco. European School of Magnetism. Cargèse (France) 2013

- Introduction
  - 5 key questions in a nutshell: What, which, where, when, why
- Optimization of soft magnetic properties
  - Coercivity: disorder is not a bad quality all the time.
  - Frequency response: losses
  - Do we always need the highest permeability?: high frequency power conversion
- Example of sensor application: GMI

Soft magnets in the global market

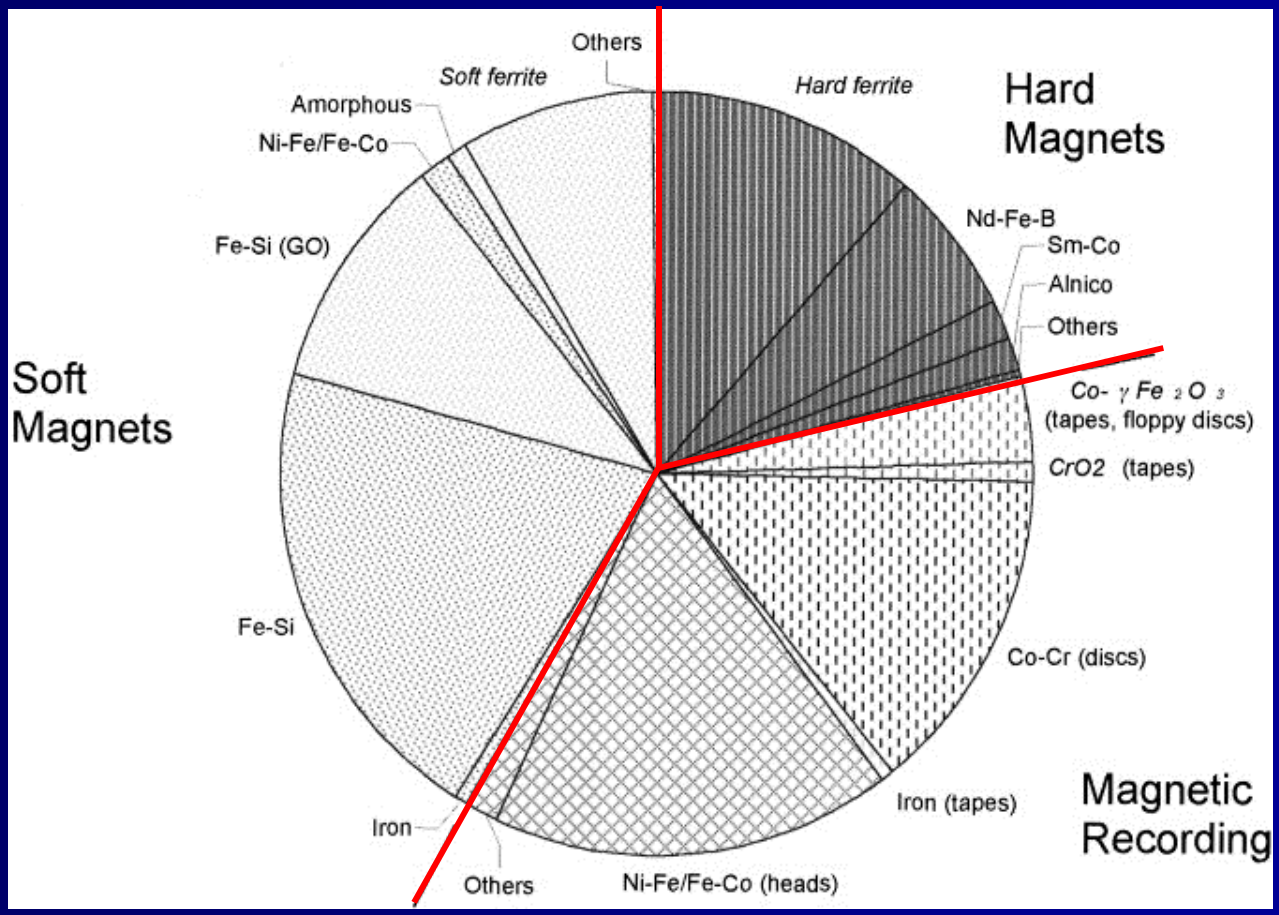

JMD Coey, J. Alloy. Compd. 326 (2001) 2

Where are they used?

- Magnetic shielding (passive)
- Flux concentrators
- Sensors, anti-theft systems
- Power conversion
  - Transformers, inductors
  - Motors, generators

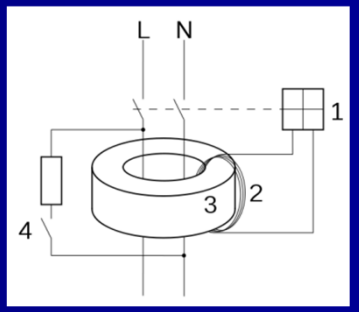

Tesla car; induction motor

What we need

- High saturation magnetization
  - composition
- Low coercivity
  - microstructure
- High Curie temperature
- High permeability (most of the times)
- Frequency response → low losses

Evolution of soft magnetic materials

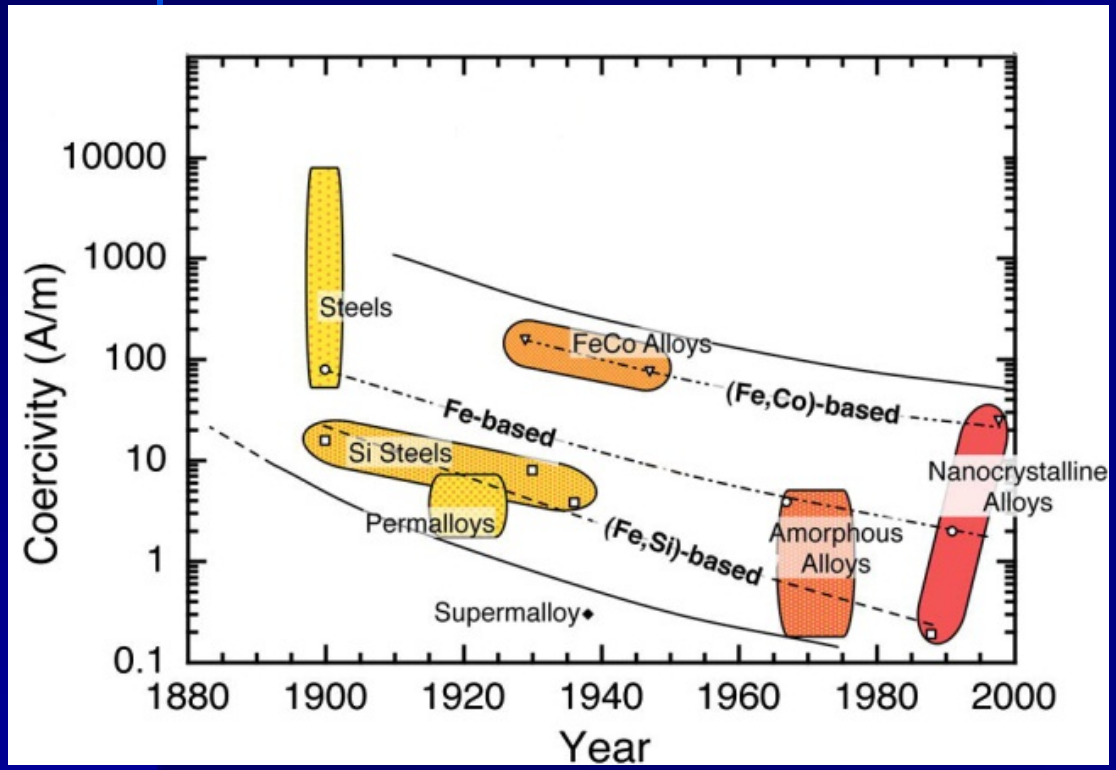

M.A. Willard, M. Daniil, K.E. Kniping, Scripta Mater. 67 (2012) 554

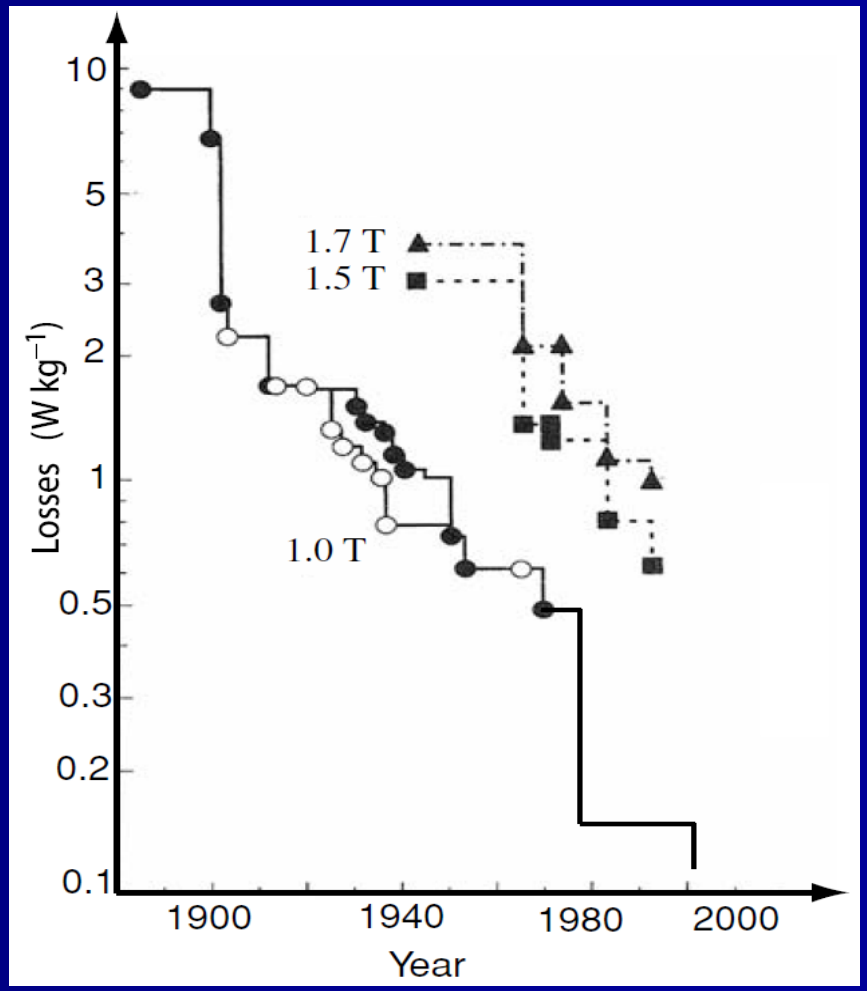

JMD Coey, Magnetism and Magnetic Materials, Cambridge University Press, 2010

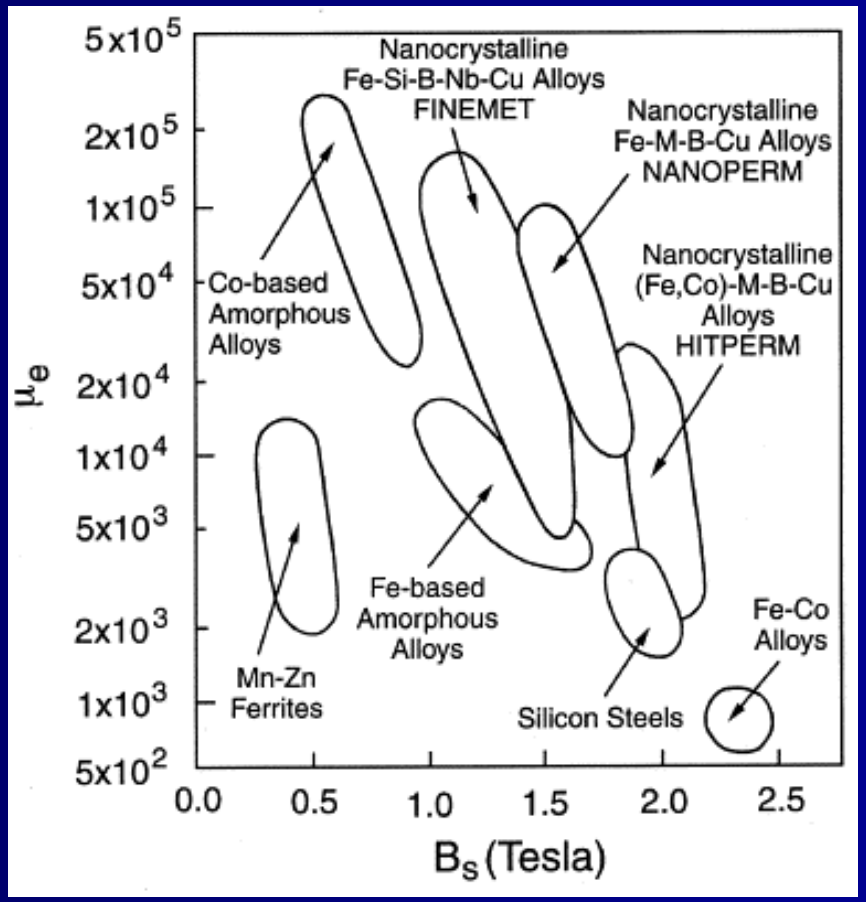

M.E. McHenry, M.A. Willard, D.E. Laughlin, Prog Mater Sci 44 (1999) 291

Warning: The importance of the demagnetizing field

$$H = H_{appl} - H_{demag}$$

$$H_{demag} = NM$$

Material:

Internal field

"intrinsic" susceptibility

$M = \chi H$

Measurement:

Applied field

Apparent susceptibility

$M = \chi_a H_{appl}$

$$\chi_a H_{appl} = \chi_a (H + NM) = \chi_a (H + N\chi H) = \chi_a H(1 + N\chi)$$

$$\chi_a = \frac{\chi}{(1 + N\chi)}$$

If N or the susceptibility are large, $\chi_a \approx 1/N$

- Small applied fields for samples with high permeability

$$\chi_a = \frac{\chi}{(1 + N\chi)} \qquad \chi_a \approx 1/N$$

$$H = H_{appl} - NM \approx H_{appl} - N(1/N\,H_{appl}) = 0$$

- M(T) for different applied fields

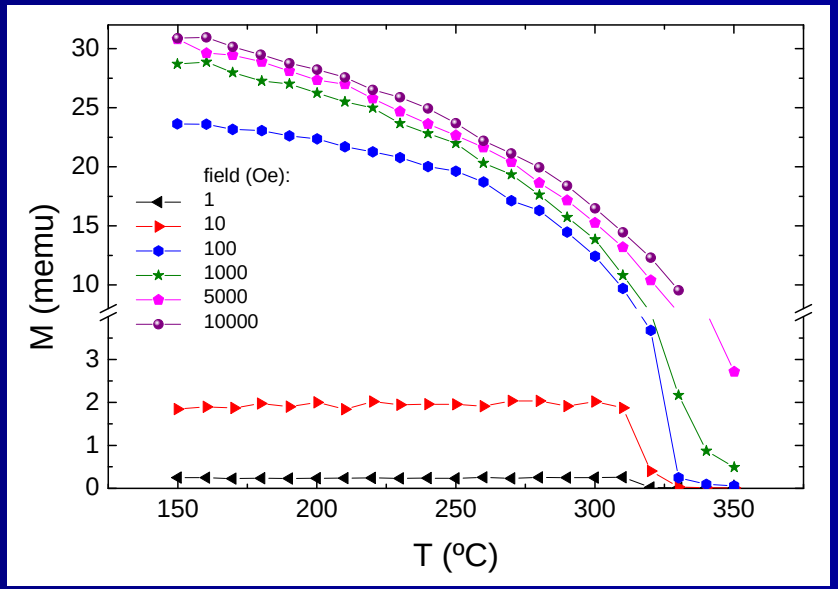

OPTIMIZATION OF COERCIVITY

Domain wall pinning and defects

- Potential energy E of the wall (per area unit):
  - Random function of position
    - Local stresses
    - Defects
- 180º domain wall of area A moving a distance x
  - Magnetization change from -M to M
  - Energy change $-2\mu_0 H_i M x$
- Equilibrium:

$$\frac{d(E-2\mu_0 H_i M x)}{dx}=0$$

$$2\mu_0 H_i M=\frac{dE}{dx}$$

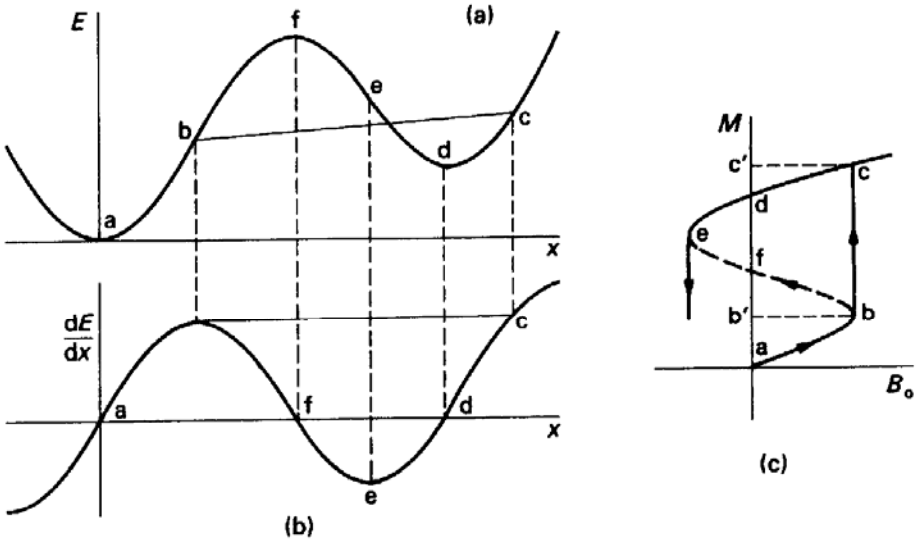

Figure 6.9 Diagrams illustrating reversible and irreversible boundary movements. Corresponding points in parts (a), (b) and (c) are marked with the same letters. (After Stoner and Rhodes, 1949, *Phil. Mag.*, **40**, 481.)

R.C. O'Handley, "Modern magnetic materials: principles and applications". John Wiley and Sons, 1999

Grain size and coercivity

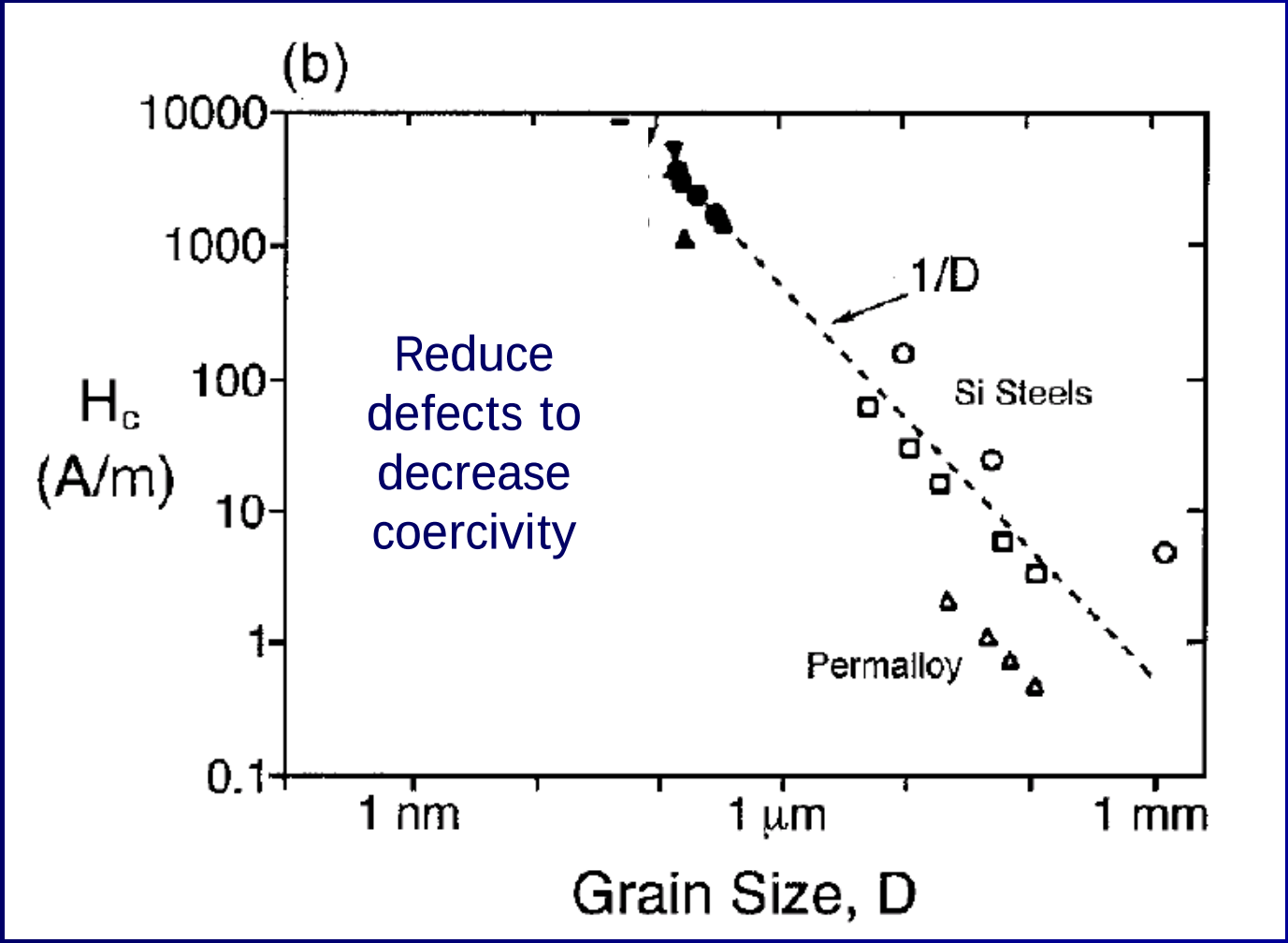

G. Herzer, J. Magn. Magn. Mater. 112 (1992) 258

Grain size and coercivity

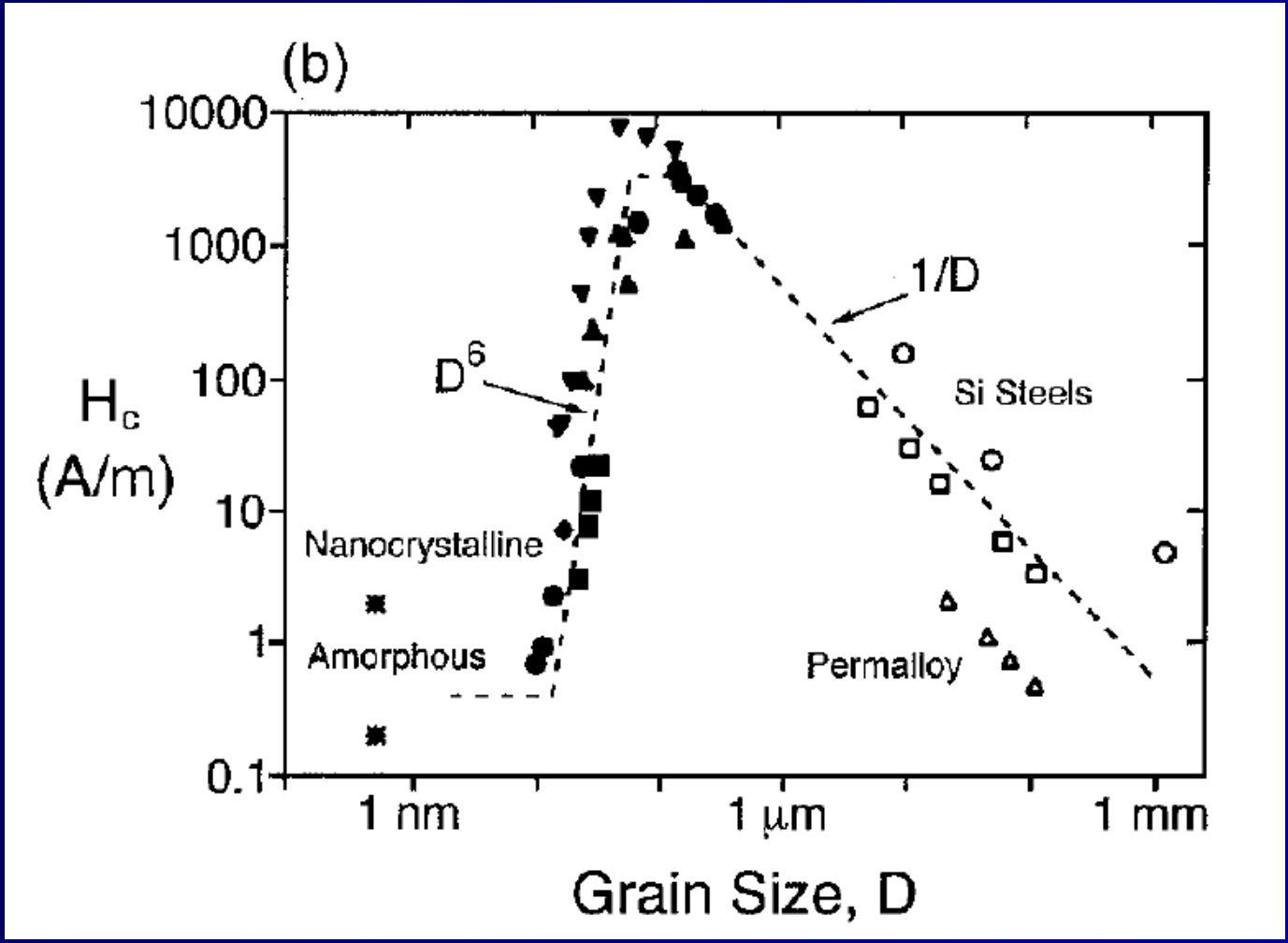

G. Herzer, J. Magn. Magn. Mater. 112 (1992) 258

SIMPLE ANALOGIES TO EXPLAIN THE SMALL CRYSTAL SIZE RANGE

(AKA: understanding the random anisotropy model without formulae)

Victorino Franco. European School of Magnetism. Cargèse (France) 2013

Who will feel the irregularities?

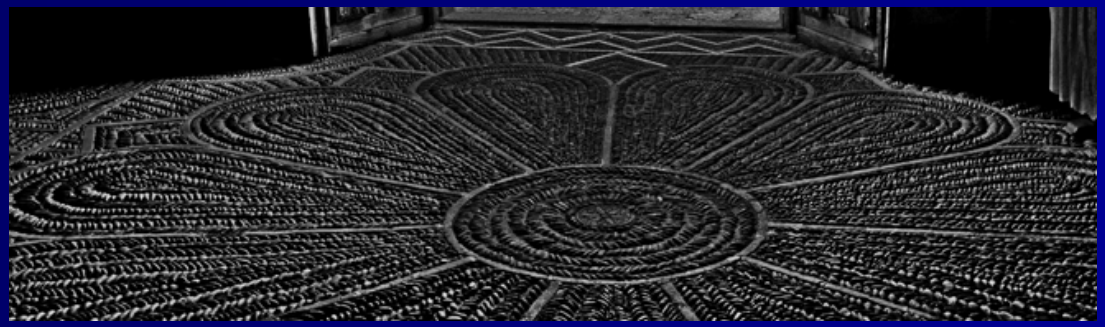

Floor of Colegiata de Santa María de Arbas, León (Spain)

The key is the different length scale (irregularities vs. shoes)

Refrigerator magnets

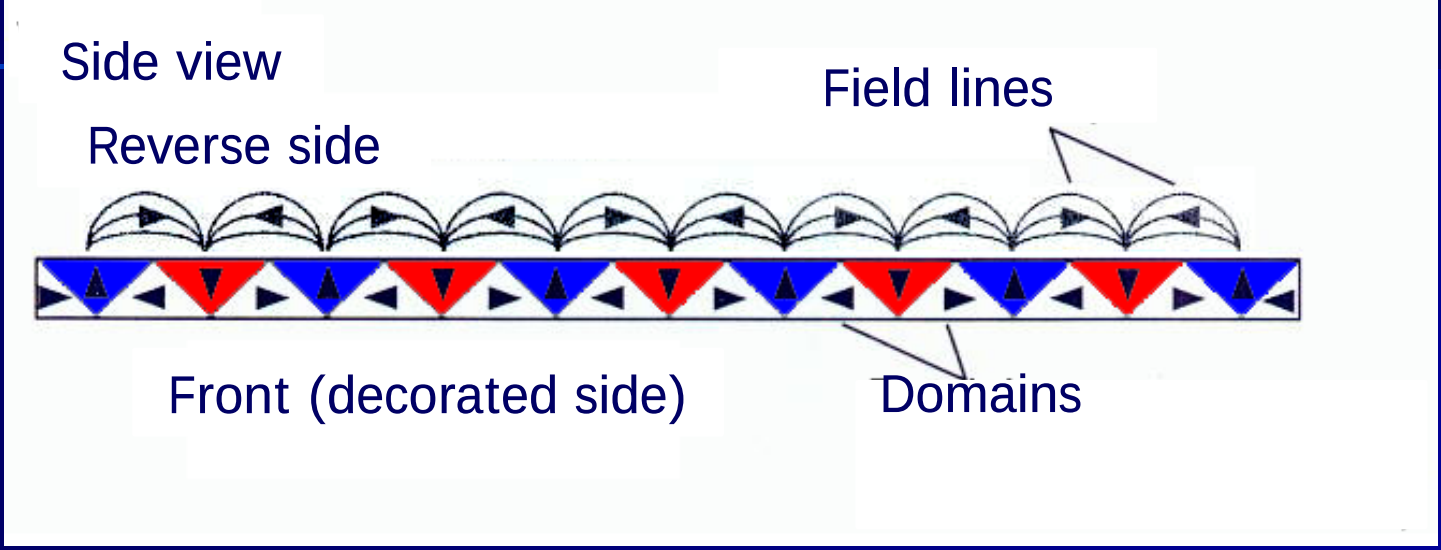

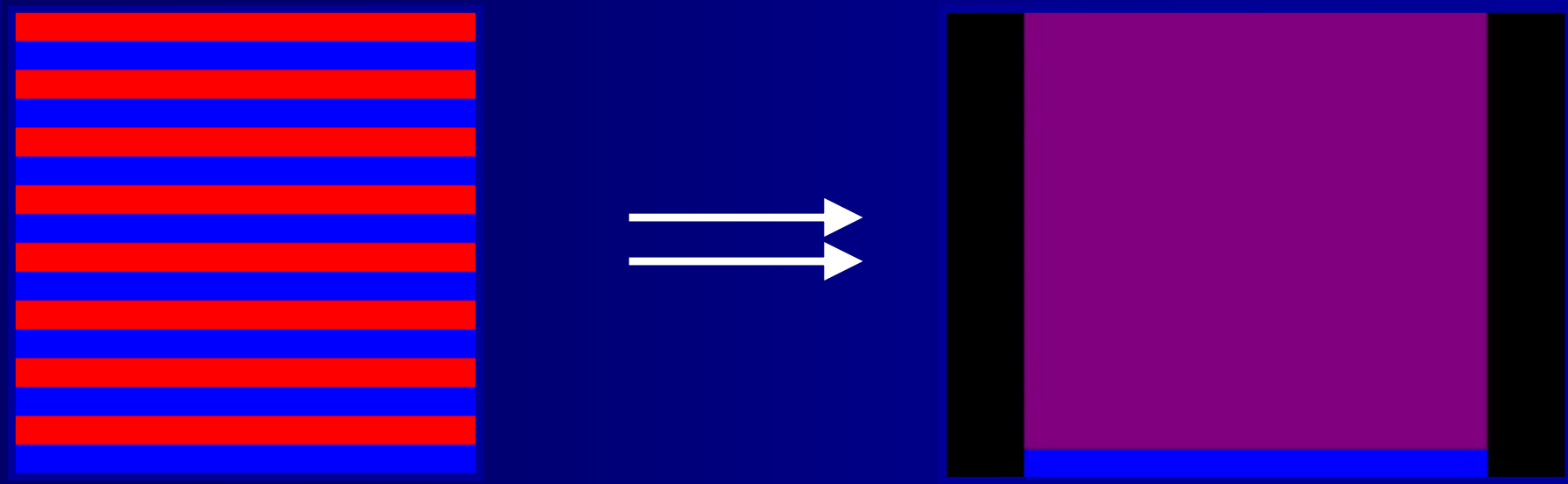

Refrigerator magnets

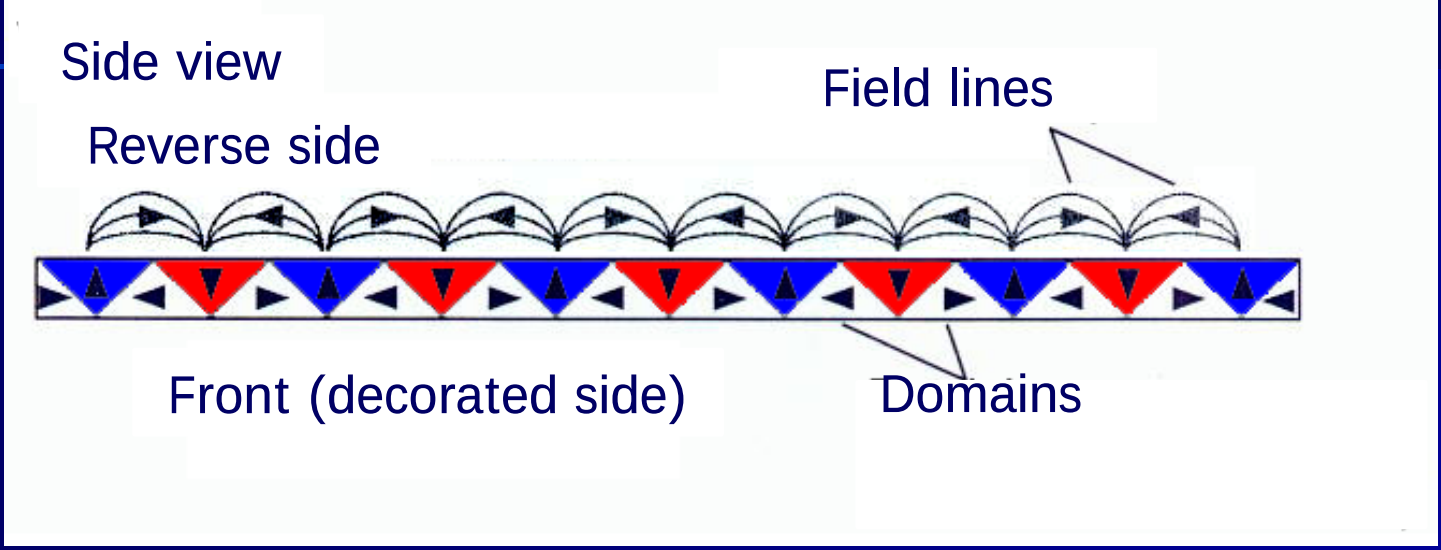

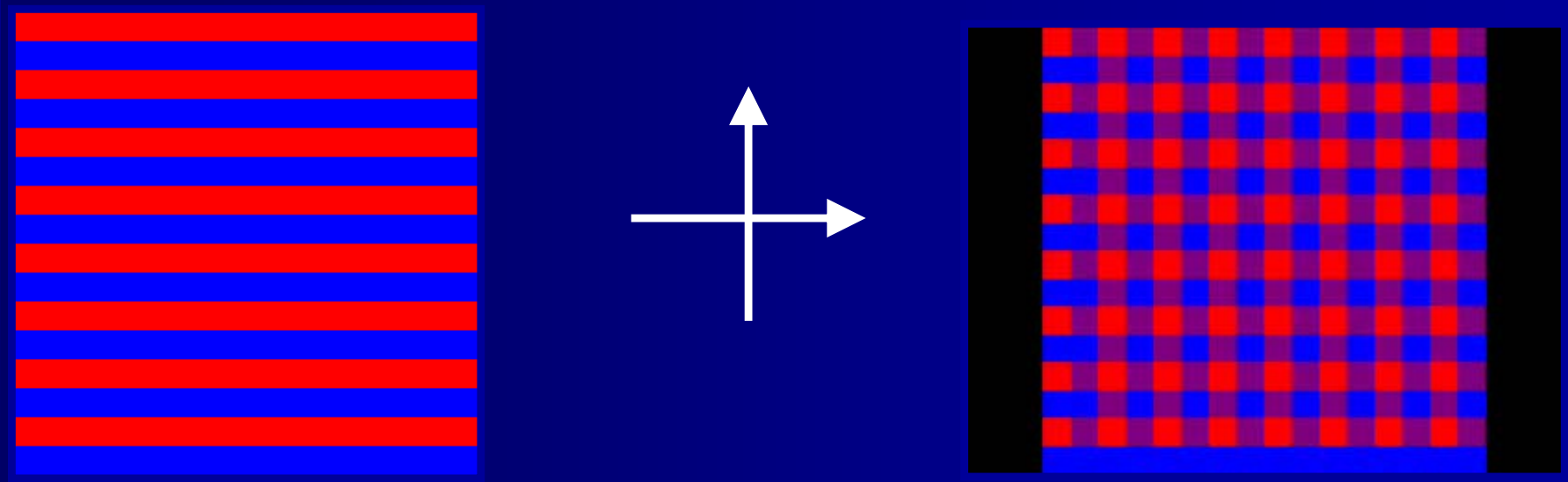

Characteristic lengths

- Two characteristic lengths along the direction of movement:
  - Substrate (separation between stripes)
  - Mobile piece
- Parallel orientations:
  - $L_{substr.}$ ~ separation between stripes
  - L_{mobile} ~ $L_{substr.}$
  - Movement significantly alters the energy of the system
- Perpendicular orientations:
  - L_{mobile} ~ size of the mobile piece
  - $L_{substr.} << L_{mobile}$
  - We cannot detect, macroscopically, energy differences

Two different correlation lengths

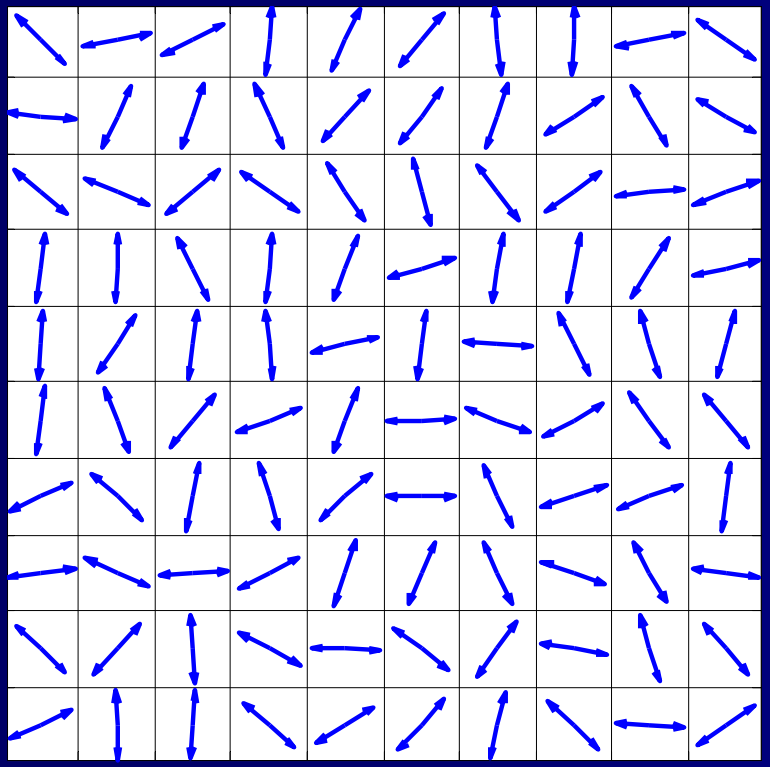

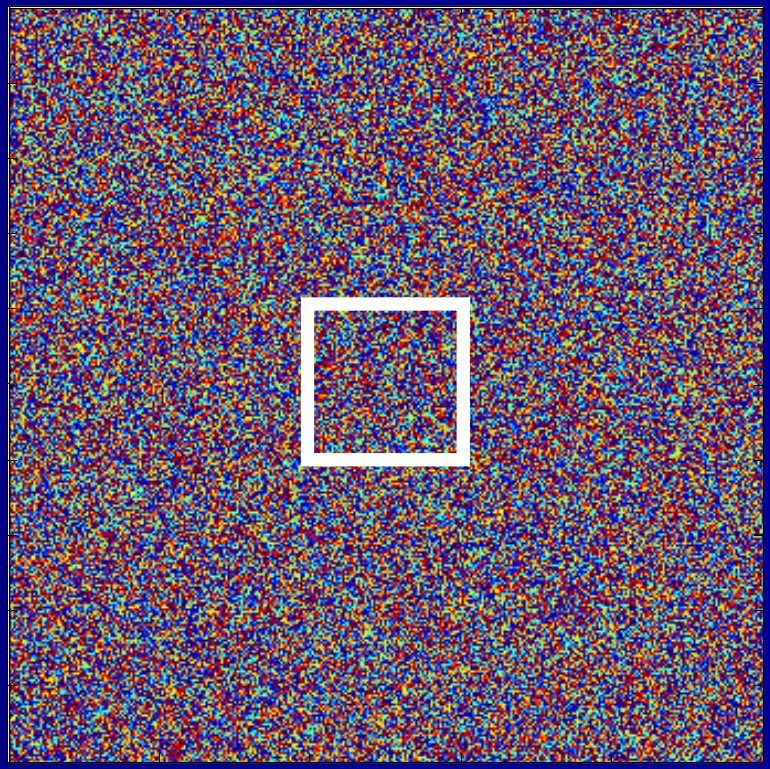

Correlation lengths

structural ⟷ magnetic

Let's quantify

- Select randomly the orientation of particles
- Choose magnetic correlated areas of different sizes
- Displace the correlated area thoughout the "sample"
- Measure the dispersion in energy
- Average multiple times

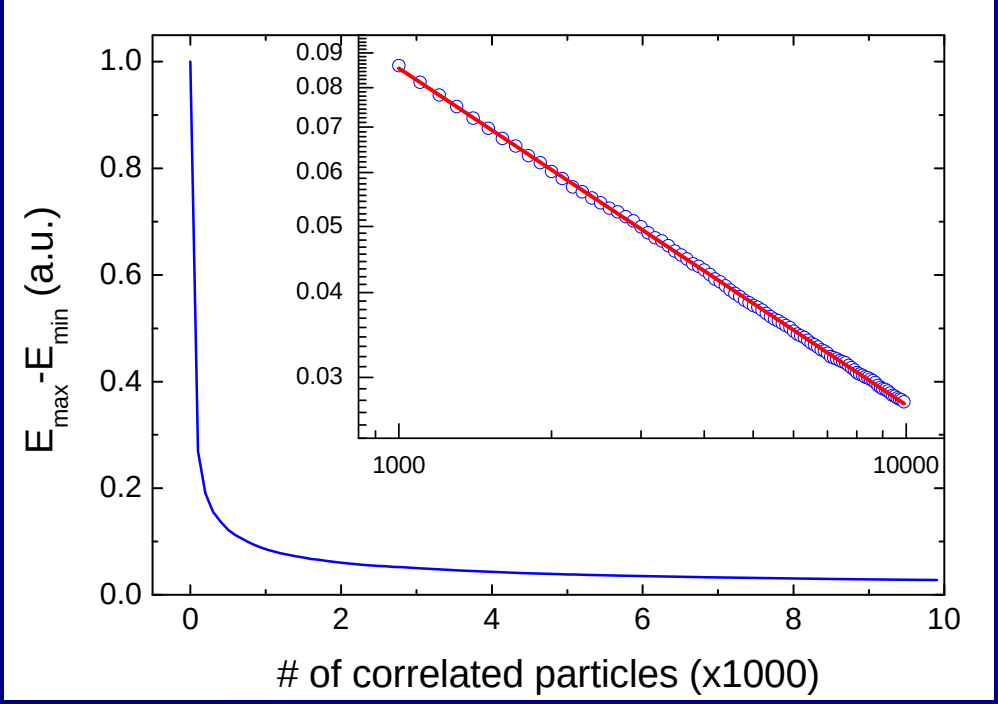

$$\propto \frac{1}{\sqrt{N}}$$

Random anisotropy model

$$K^* = \frac{K}{\sqrt{N}}$$

$$N = \left(\frac{L}{l}\right)^3$$

$$K^* \propto K^4 l^6 / A^{*3}$$

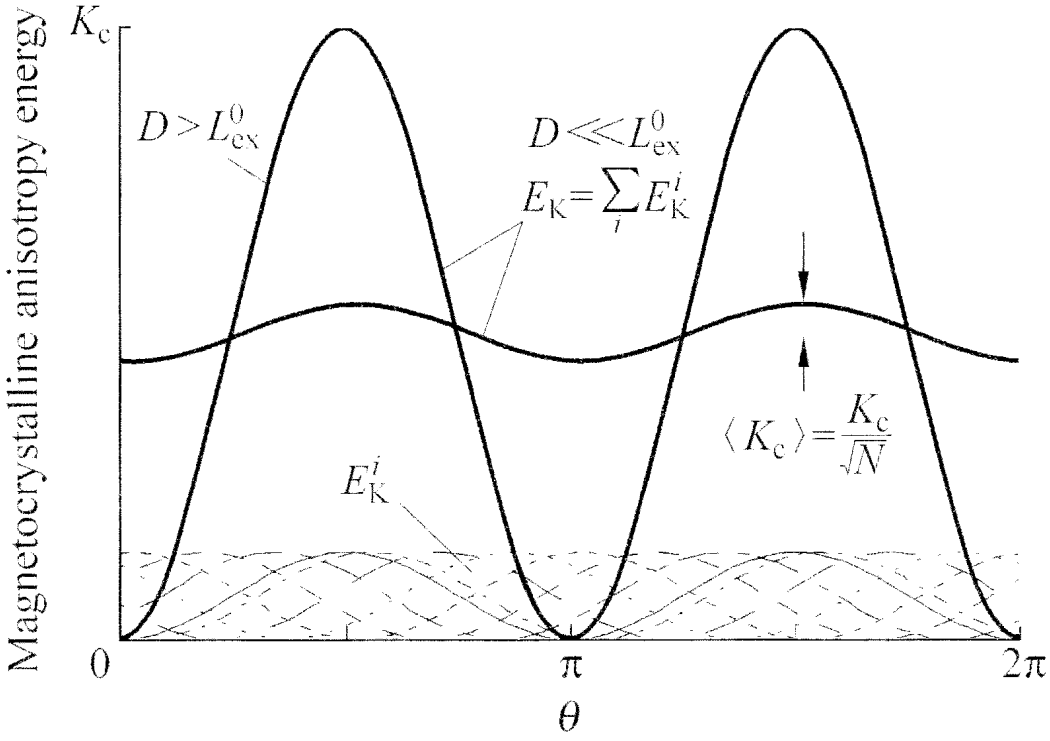

G. Herzer, J. Magn. Magn. Mater. 112 (1992) 258

K. Suzuki, in Handbook of Advanced Magnetic Materials, Springer, 2006, pp. 339-373

Finemet alloy

- Composition: $Fe_{73.5}Si_{13.5}B_9Cu_1Nb_3$
- Magnetically softer after nanocrystallization
  - Two phase nature
  - Influence of the addition of Cu & Nb
    - Segregation of Cu-rich clusters
    - Rejection of Nb at the crystal interfaces
- Importance
  - Technological applications (magnetic sensors, anti-theft systems, etc.)
  - Fundamental studies in magnetism

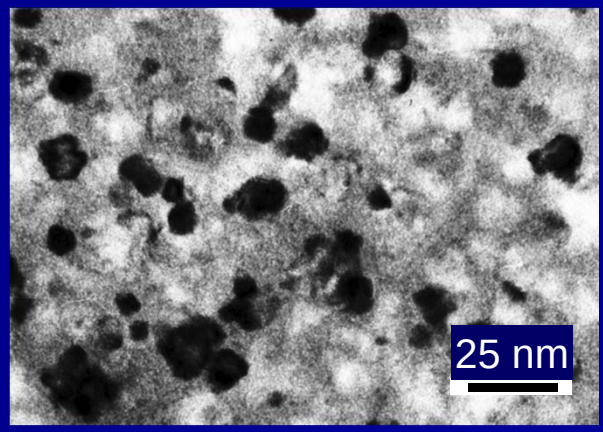

Production of amorphous alloys I: melt spinning

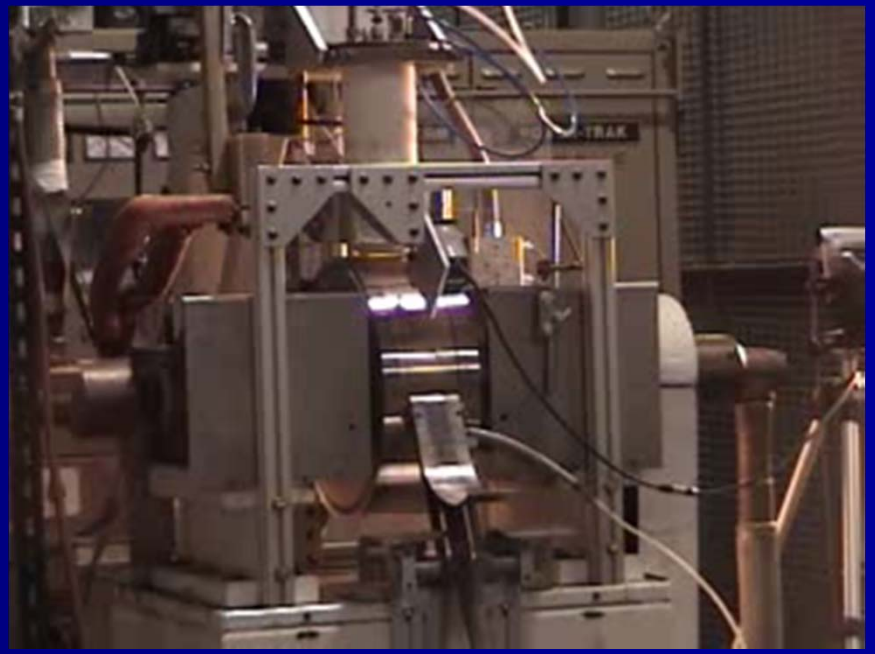

Video courtesy of Joseph F. Huth III
MAGNETICS, div. of SPANG & CO.

Crystallization behavior

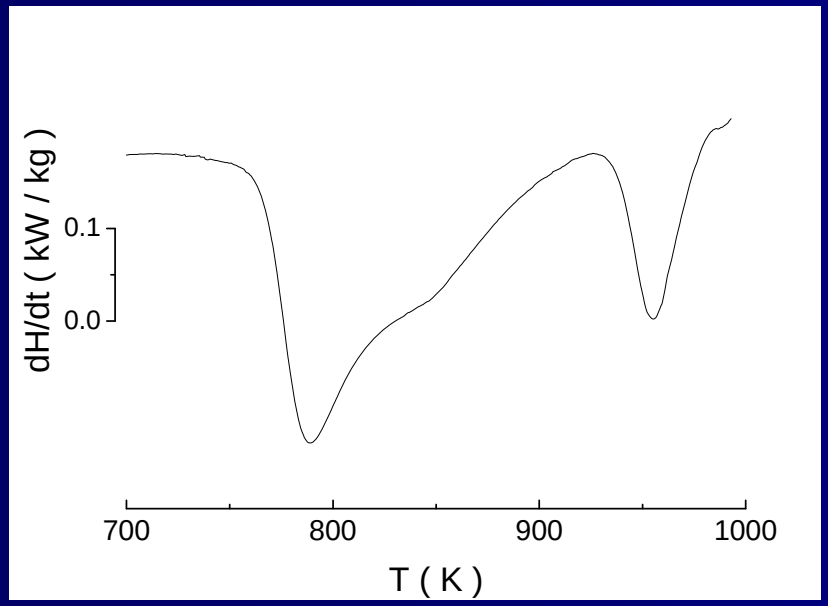

$Fe_{76}Si_{10.5}B_{9.5}Cu_1Nb_3$

- Devitrification takes place in two main stages
  - 1st exotherm: α-Fe,Si
  - 2nd exotherm: Fe_2B, ...
- Compositional effects
  - Substitution of Fe by Cr or Mo
    - Enhancement of the stability of the amorphous phase

Microstructure

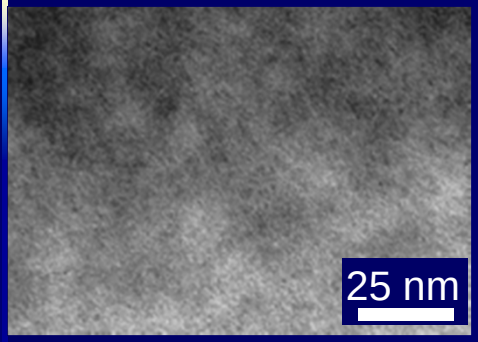

Amorphous

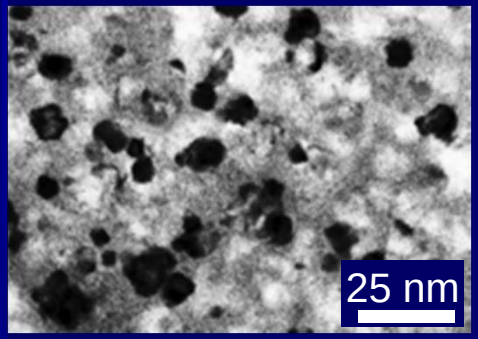

Nanocrystalline

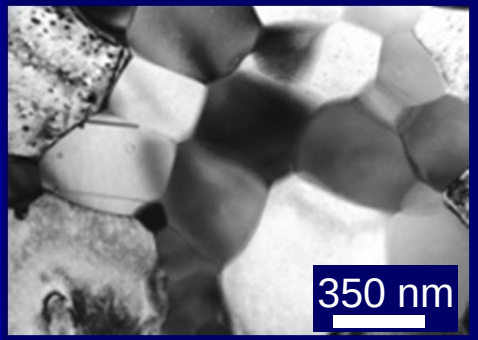

Fully crystallized

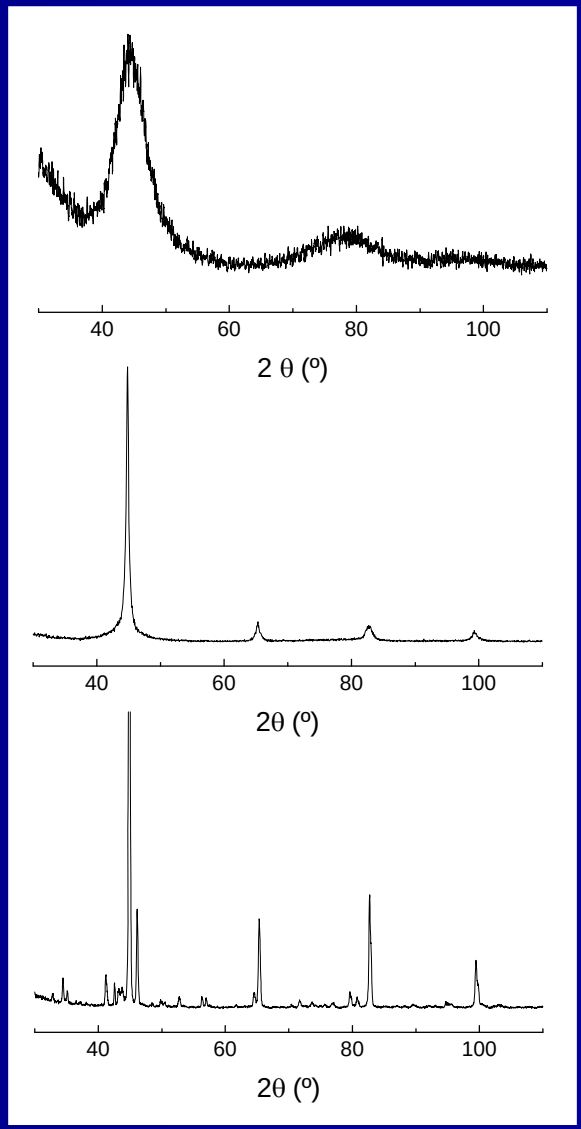

Thermomagnetic measurements

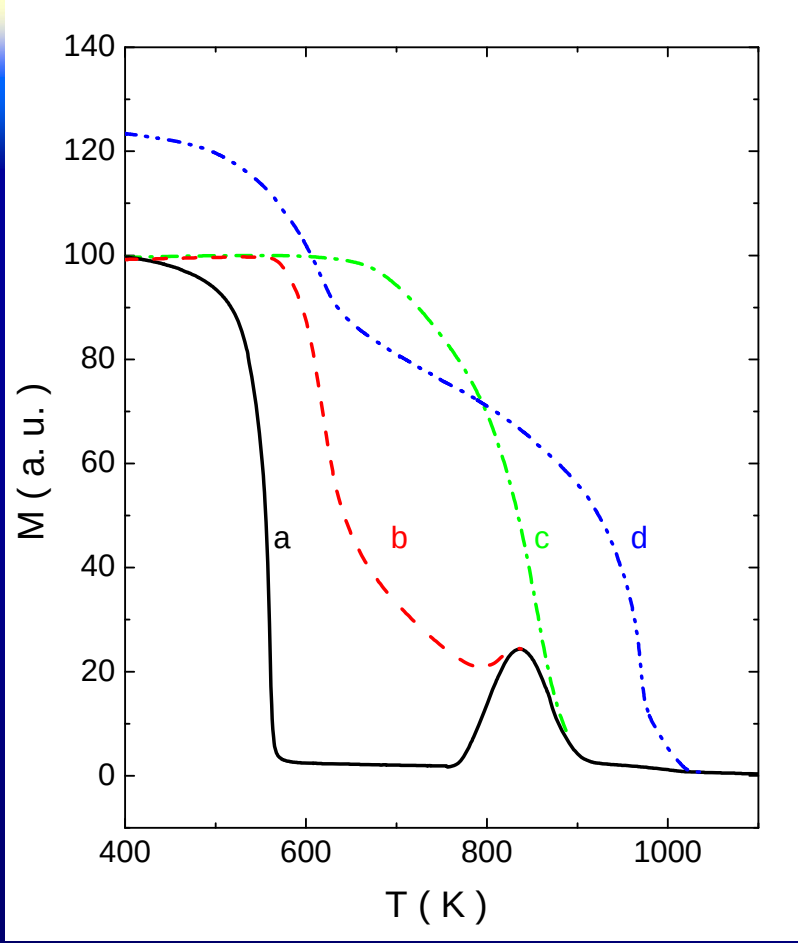

- As cast sample (a):
  - T_c(Amorphous)
  - Onset of Crystallization
  - T_c(Fe,Si)
- Nanocrystalline (b,c):
  - T_c(residual amorphous)
  - T_c(Fe,Si)
- Fully crystallized (d):
  - T_c(Fe,Si) (change in % Si)
  - T_c(Fe_2B)
  - T_c(boride type phase)

V. Franco, C.F. Conde, and A. Conde, J. Magn. Magn. Mater. 185 (1998) 353

Coercivity

2nd crystallization stage

Nanocrystallization onset

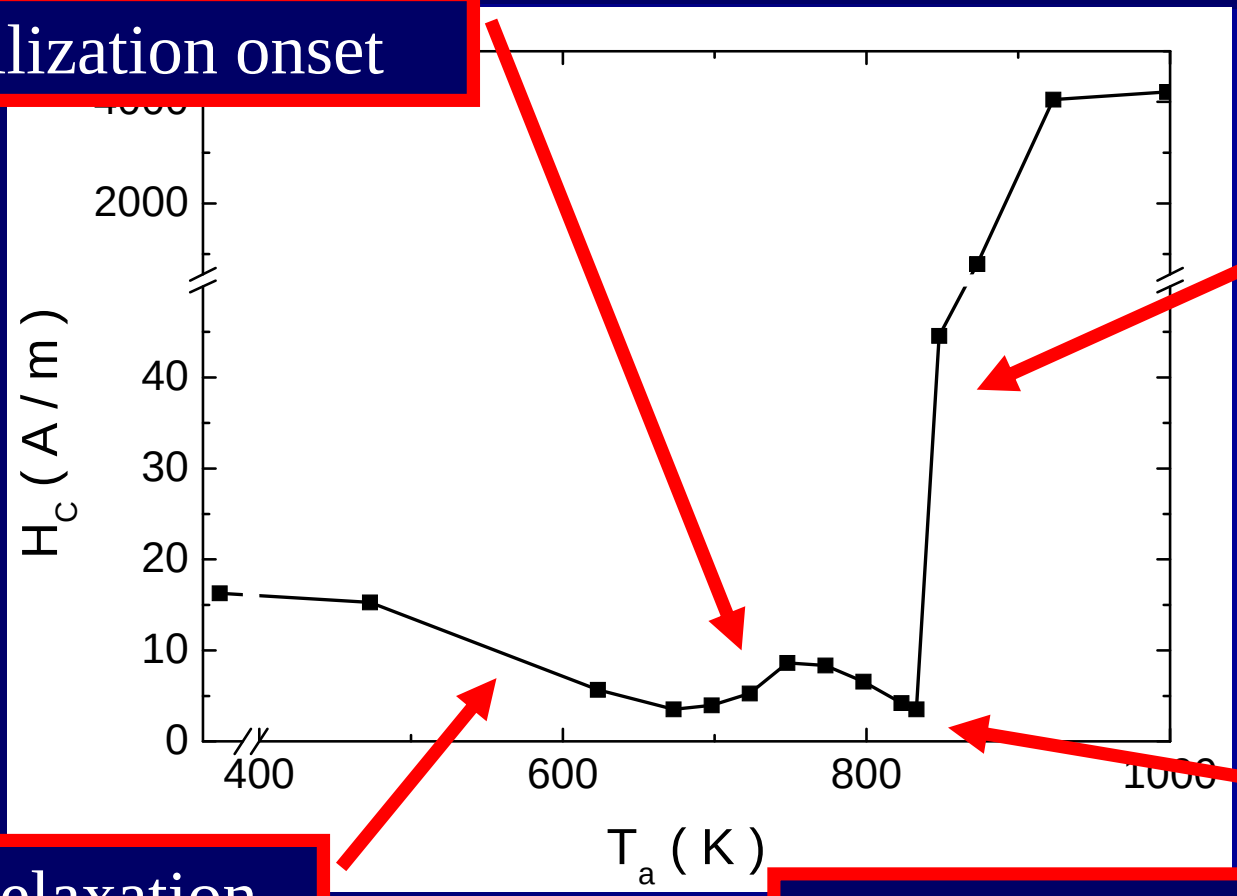

Stress relaxation

Averaging of anisotropy

V. Franco, C.F. Conde, A. Conde, L.F. Kiss, J. Magn. Magn. Mater. 215 (2000) 400

High temperature soft magnetic nanocrystalline alloys

- Can we keep the soft magnetic properties at higher temperatures? Limitations:
  - Microstructural evolution
  - Magnetic softness
- Individual nanoparticles
  - Superparamagnetism
    - No hysteresis
    - Overlapping of magnetization curves $M = N\mu L\left(\frac{\mu_0 \mu H}{kT}\right)$
    - Limited by anisotropy energy (T_B)
- Nanocrystalline alloys?

Superparamagnetism in nanocrystalline alloys

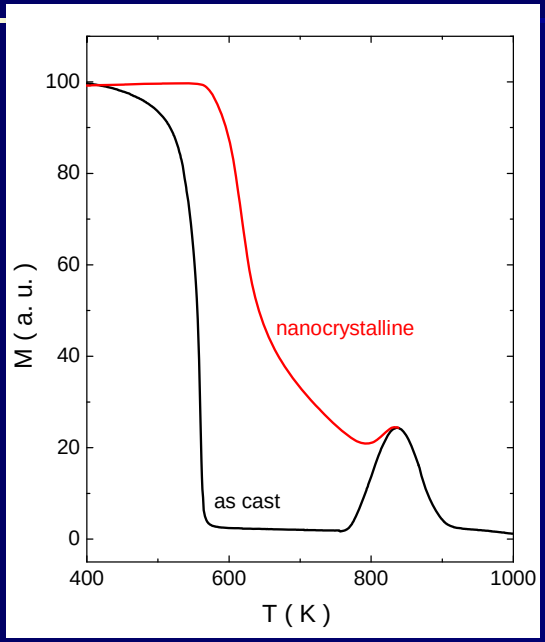

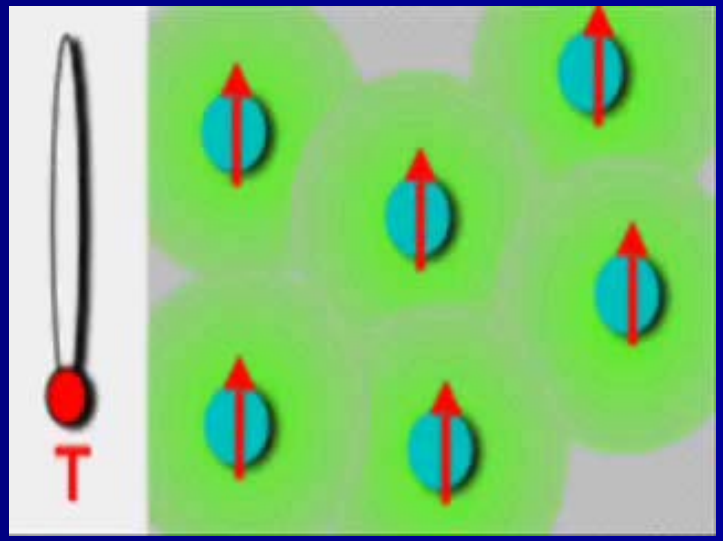

- Low temperature: blocked state (ferromagnetic matrix)
- High temperature: superparamagnetic relaxation
  - Not controlled by blocking temperature, but by the ferromagnetism of the matrix

Superparamagnetic relaxation

$$M = N\mu L\left(\frac{\mu_0 \mu H}{kT}\right)$$

- Requisites:
  - No hysteresis
  - Overlapping of magnetization curves
- Limited by:
  - Anisotropy energy (T_B)
  - Decoupling of the grains
  - 2nd crystallization stage

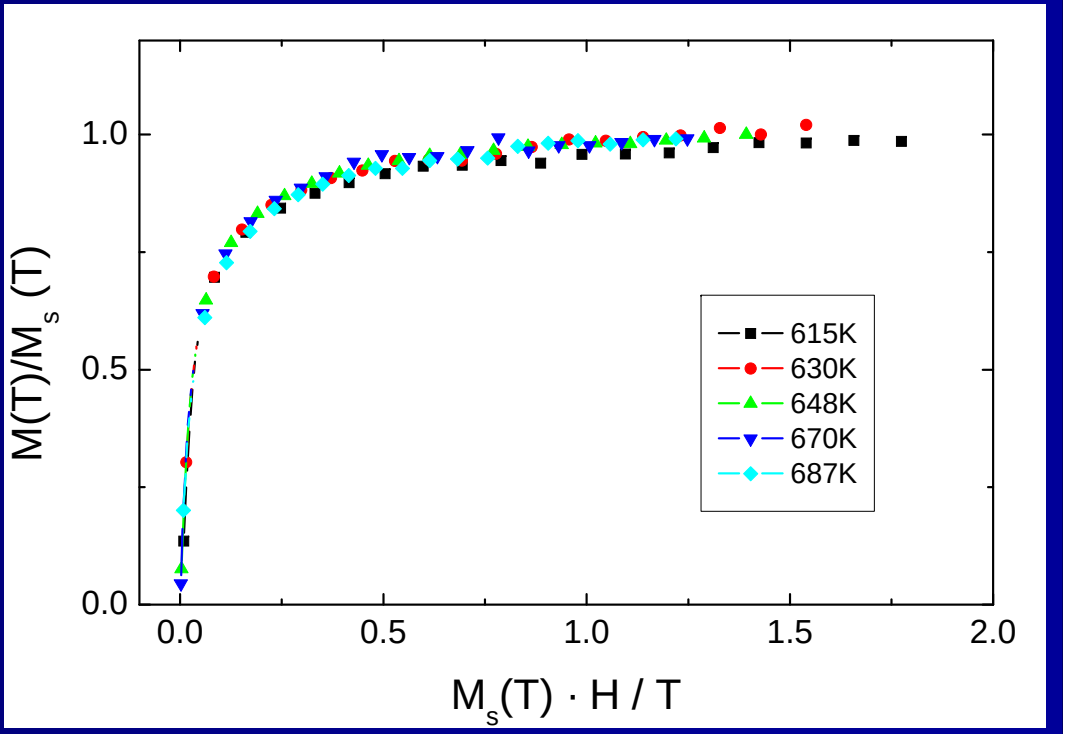

V. Franco, C.F. Conde, A. Conde, L.F. Kiss, J. Magn. Magn. Mater. 215 (2000) 400

Cr-containing Finemet alloy

$Fe_{63.5}Cr_{10}Si_{13.5}B_9Cu_1Nb_3$

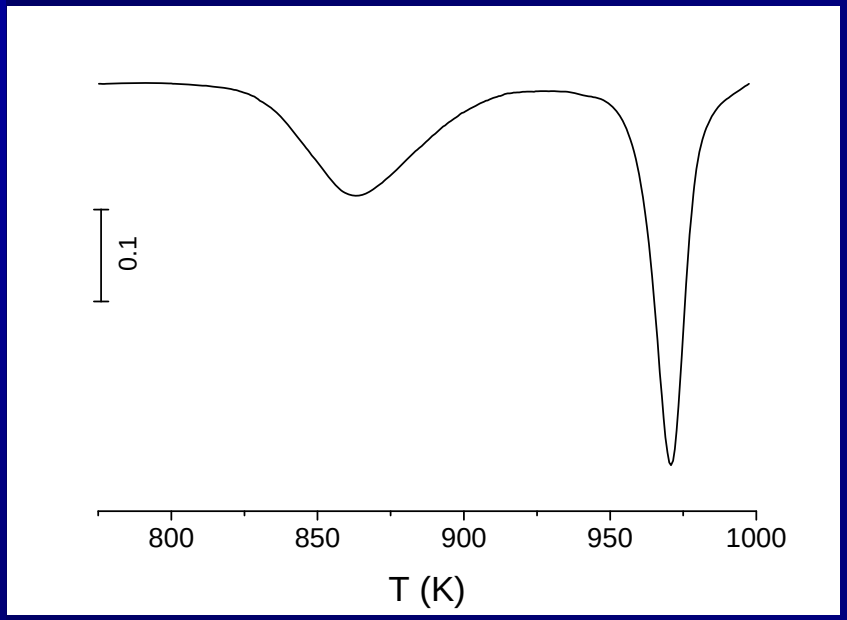

- Thermal stability is enhanced
- Cryst. volume fraction is reduced
- Smaller mean grain size

V. Franco et al., J. Appl. Phys. 90 (2001) 1558

Thermomagnetic properties

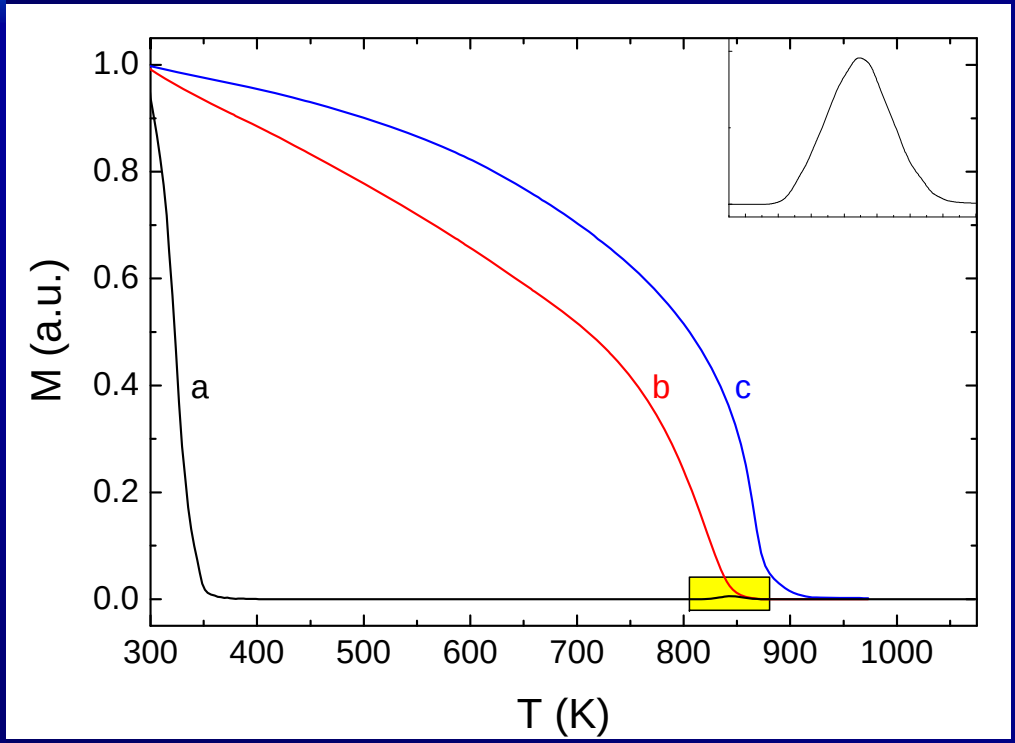

- Significant reduction of T_c^{am}
- Nanocrystallization onset is less detectable
- T_c (rem. am.)?

V. Franco, C.F. Conde, A. Conde, J. Magn. Magn. Mater. 203 (1999) 60

Thermomagnetic properties (low T)

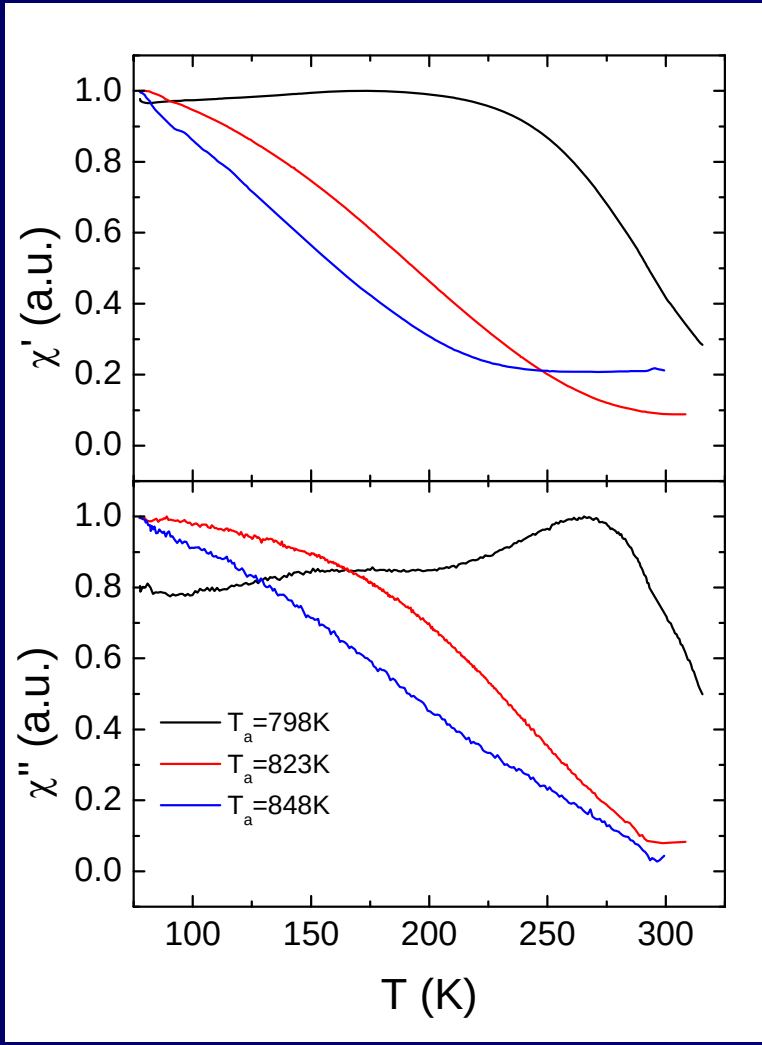

- T_c(rem. am.) is reduced with increasing T_a
  - Grains should be easily decoupled

Hysteresis loops

Averaging of anisotropy?

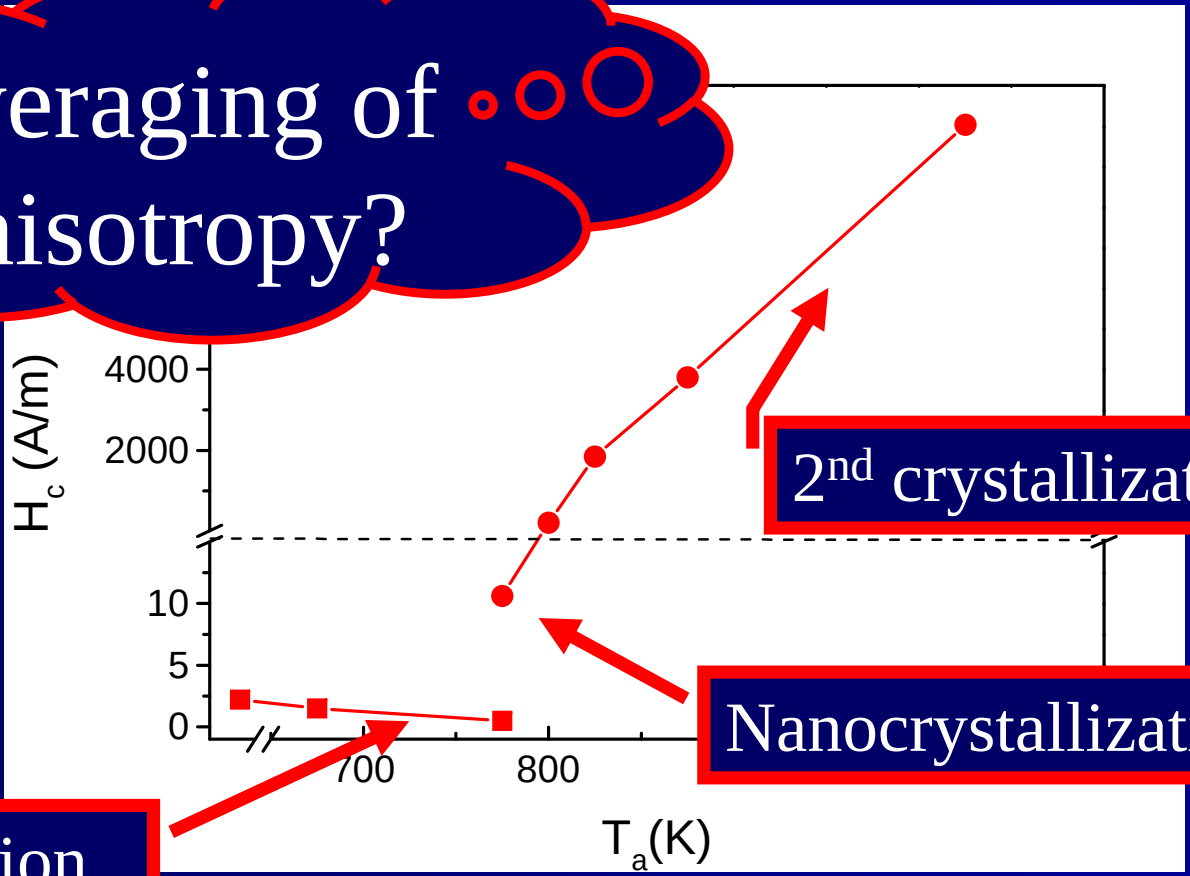

2nd crystallization stage

Nanocrystallization onset

Stress relaxation

V. Franco et al., IEEE Trans. Mag. 38 (2002) 3069

Hysteresis loops

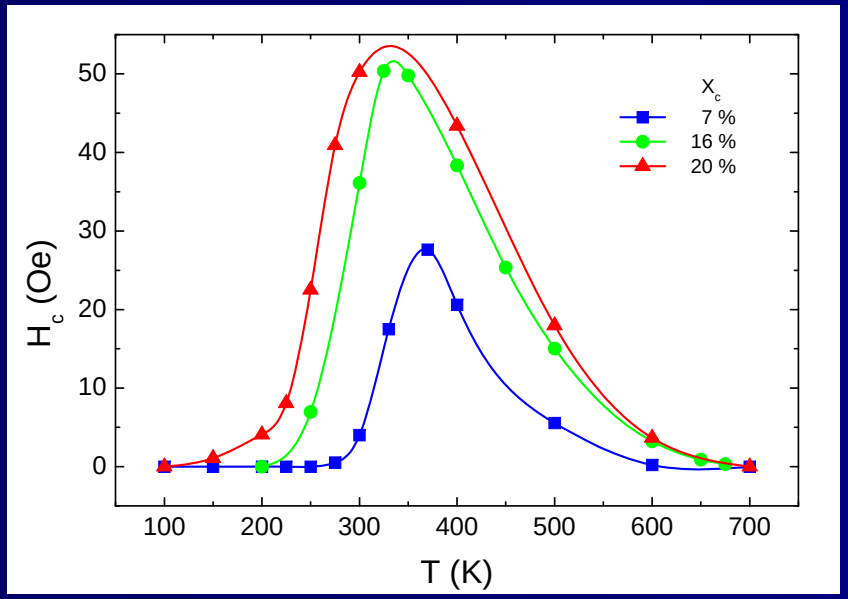

- Coercivity has a maximum around room temperature
- It is displaced to lower temperatures as crystalline volume fraction increases
  - T_c(res. Am.)

V. Franco et al., Phys. Rev. B 66 (2002) 224418

Superparamagnetic relaxation

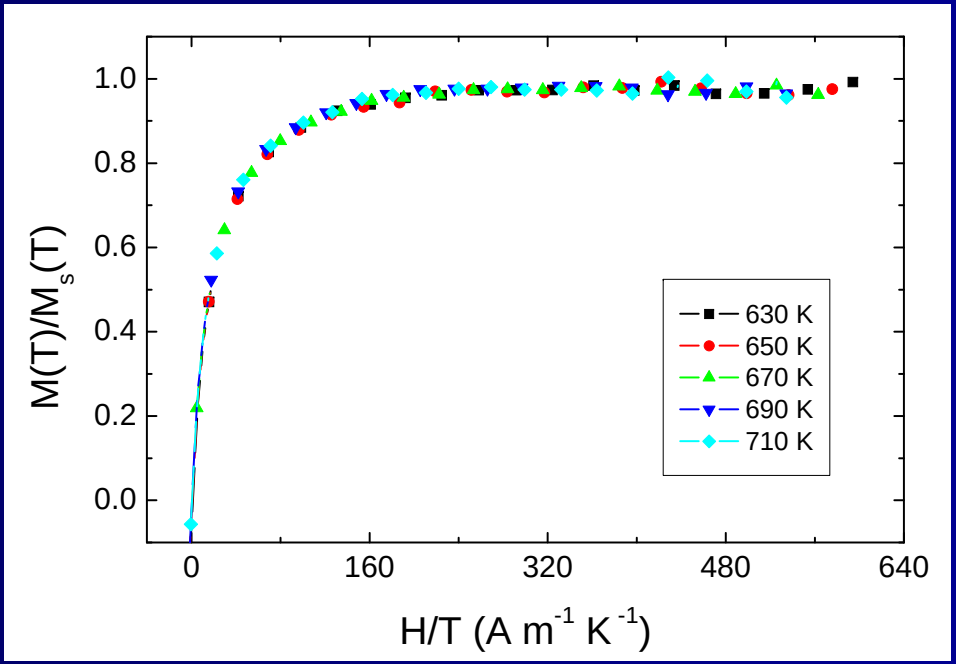

T_a	p_x	D_x (nm)	$\langle\mu\rangle$ (103 μ_B)	D (nm)
775 K	undetectable	undetectable	18 ± 7	5.2 ± 0.7
800 K	0.066	9 ± 2	41 ± 6	6.8 ± 0.5
825 K	0.197	12 ± 2	112 ± 6	9.6 ± 0.5
850 K	0.385	13 ± 2	113 ± 6	9.6 ± 0.5

V. Franco et al., J. Appl. Phys. 90 (2001) 1558

Dipolar interactions between SPM nanoparticles

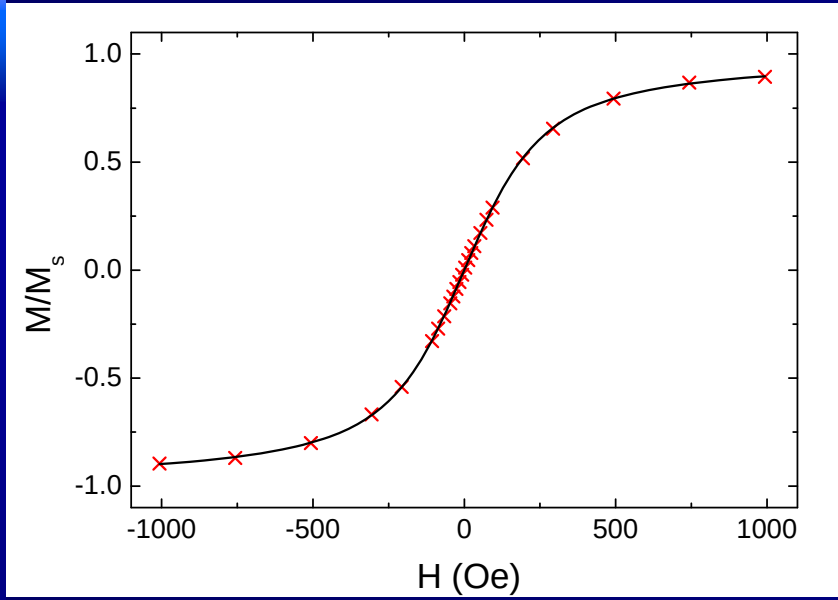

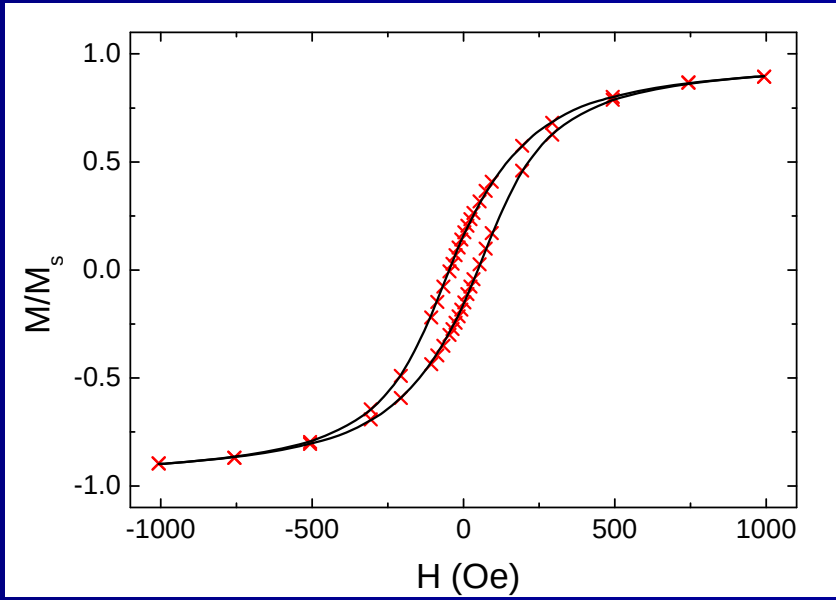

Sample with p_x=20 %, measured at 400 K

$$\mu_{app} = \frac{1}{1+T^*/T}\,\mu \qquad M = N\,\mu\,L\left(\frac{\mu\ H}{k\ (T+T^*)}\right) \qquad kT^* = \xi\mu H_0$$

V. Franco et al., Phys. Rev. B 66 (2002) 224418; Phys. Rev. B 72 (2005) 174424

Production of amorphous alloys II: mechanical alloying

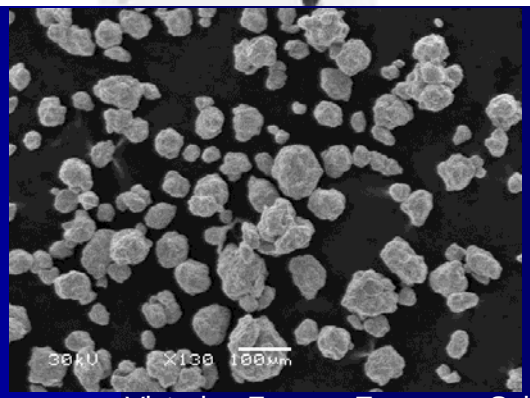

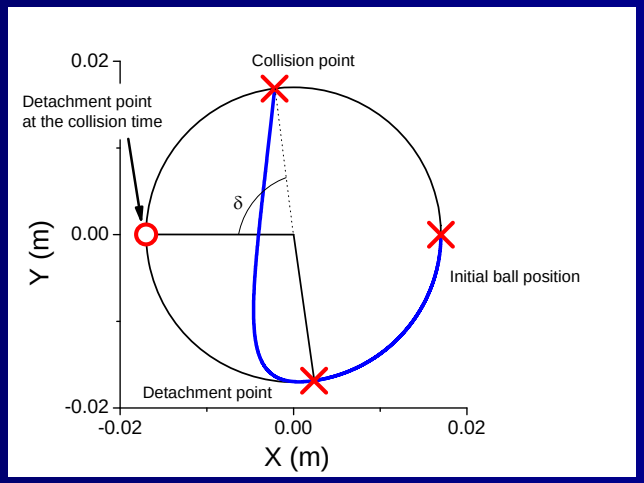

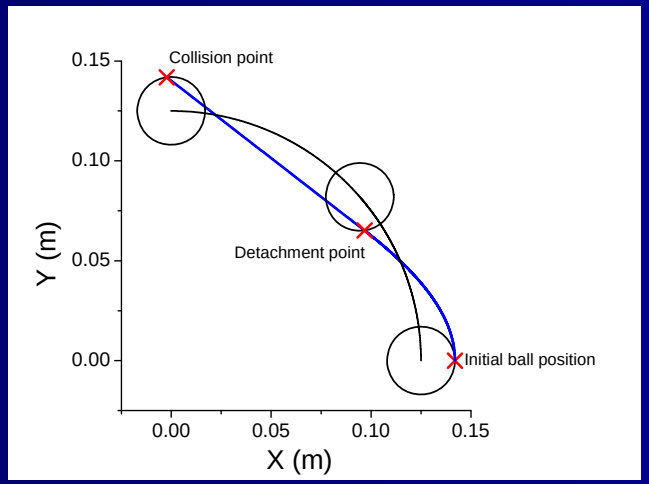

Ipus et al, Intermetallics 16 (2008) 470

- Powders can be compacted to obtain the final shape
- For the same nominal composition, properties are different from those of melt spun alloys

Influence of the starting phases

$Fe_{75}Nb_{10}B_{15}$ composition prepared using:

- crystalline boron (c-B alloy)
- amorphous boron (a-B alloy)

$(Fe_{75}Nb_{10})_{100}$ composition (n-B alloy)

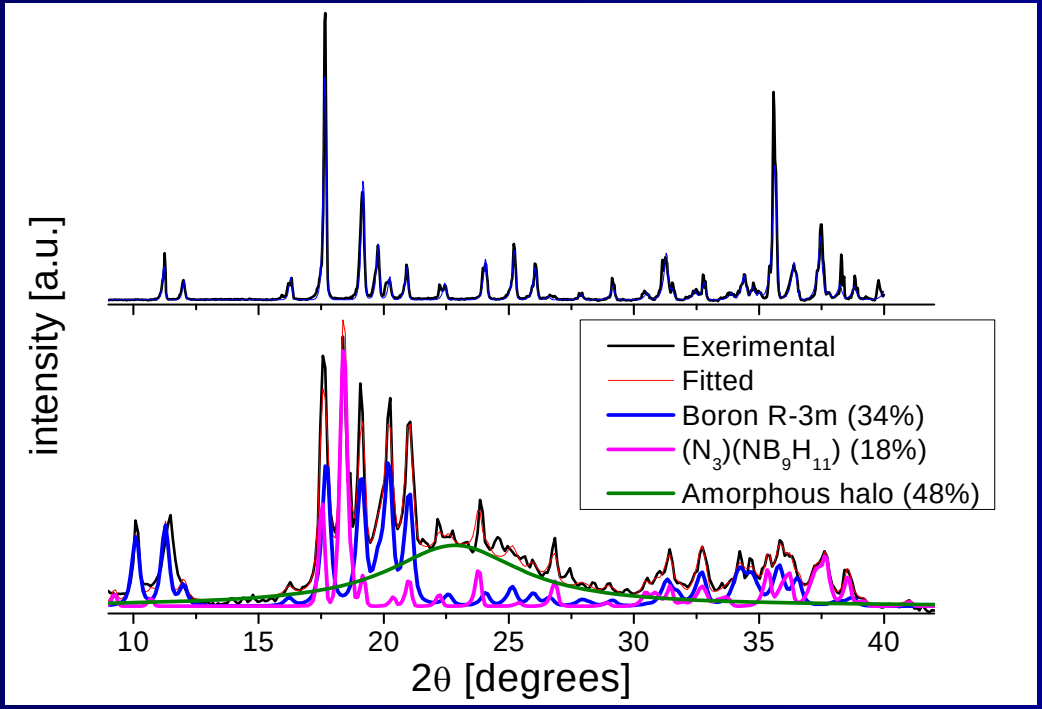

Crystalline boron

Commercial amorphous boron

J.J. Ipus, J.S. Blázquez, V. Franco, A. Conde, J. Appl. Phys. 113 (2013) accepted

Global microstructure I XRD patterns

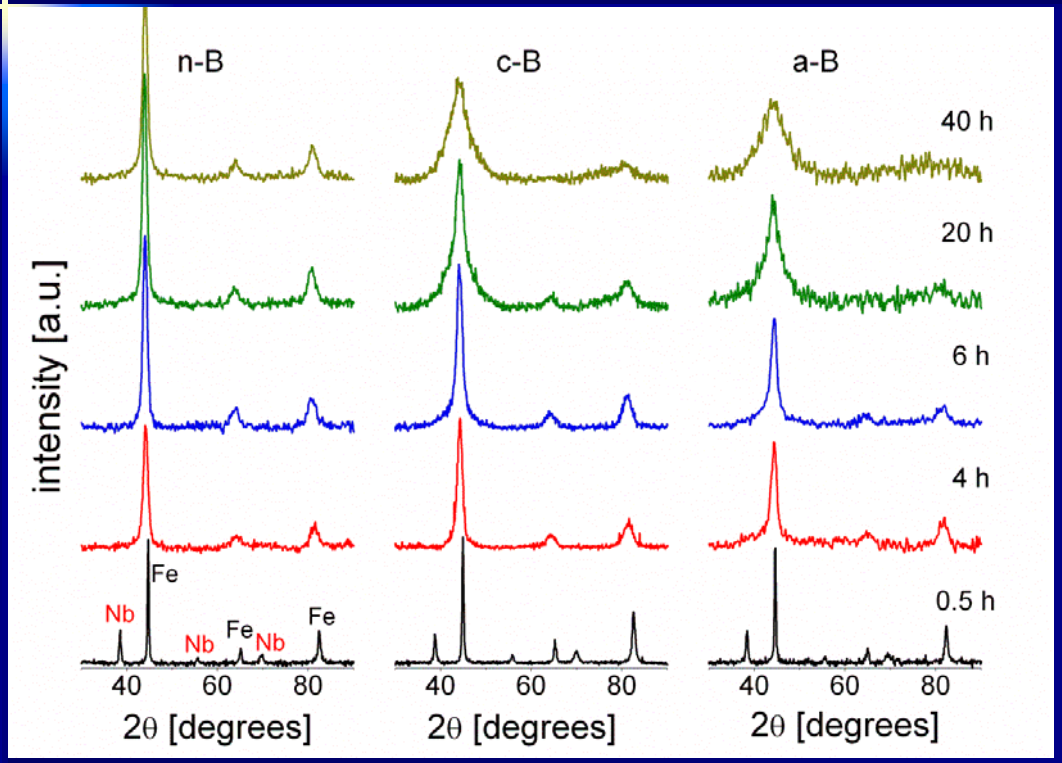

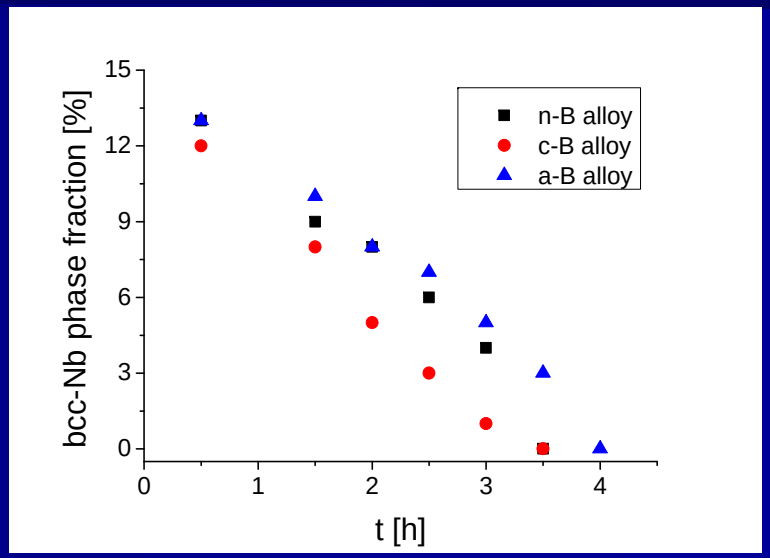

- Bcc Nb phase dissapears after 4 h miling
- Amorphous phase developed only in B containing alloys

XRD results

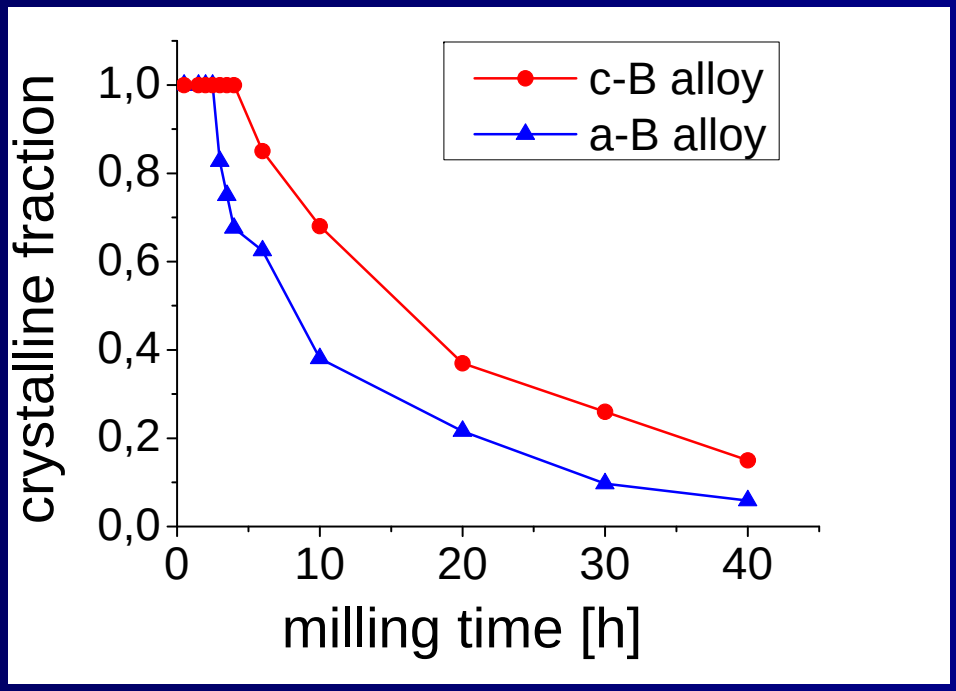

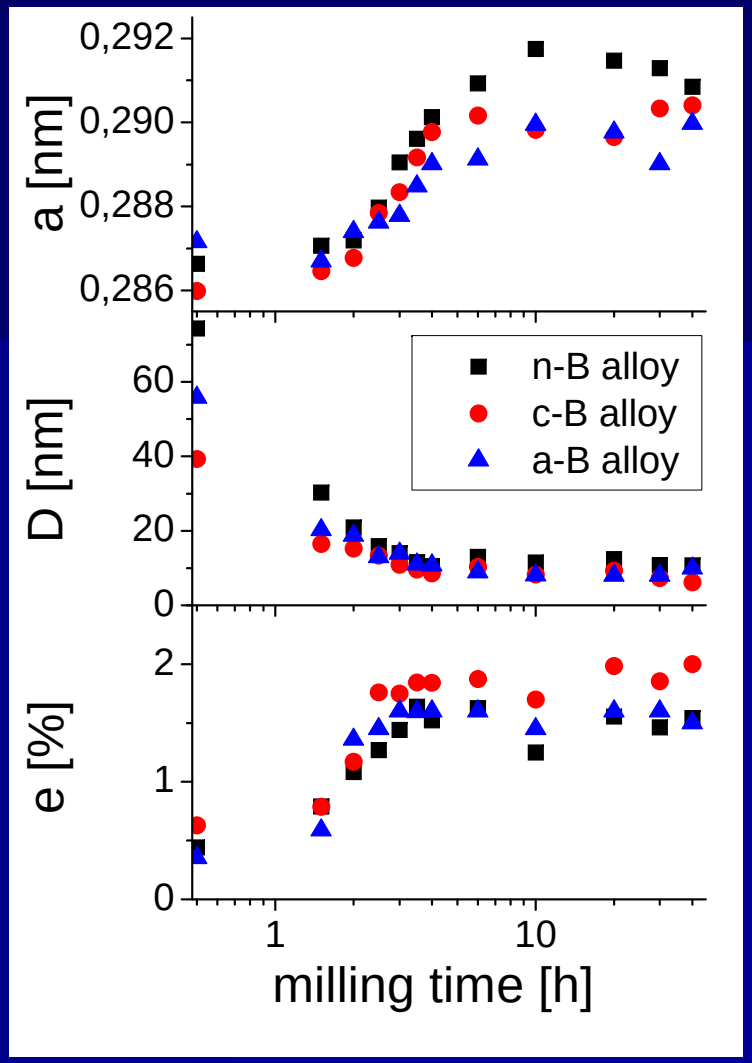

- Faster amorphization in a-B alloy
- Microstructural parameters of crystalline phase almost stabilized after 4 h milling

TEM sample preparation

(Focused Ion Beam)

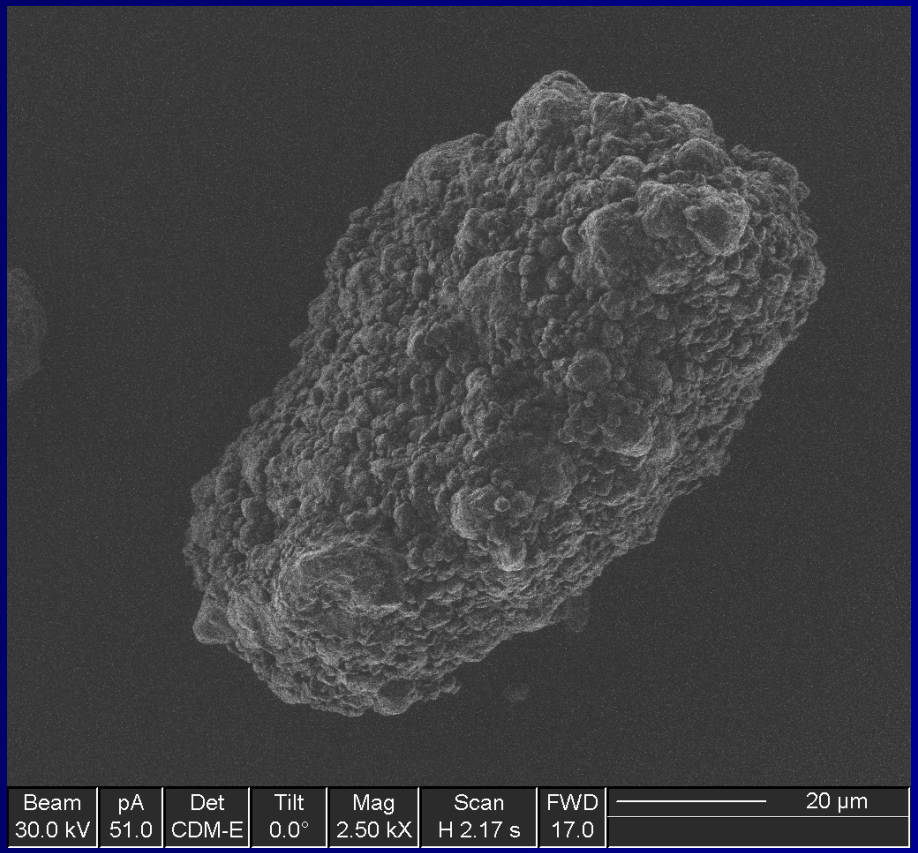

Powder particle selected

Ipus et al, Phil. Mag. 89 (2009) 1415

TEM sample preparation

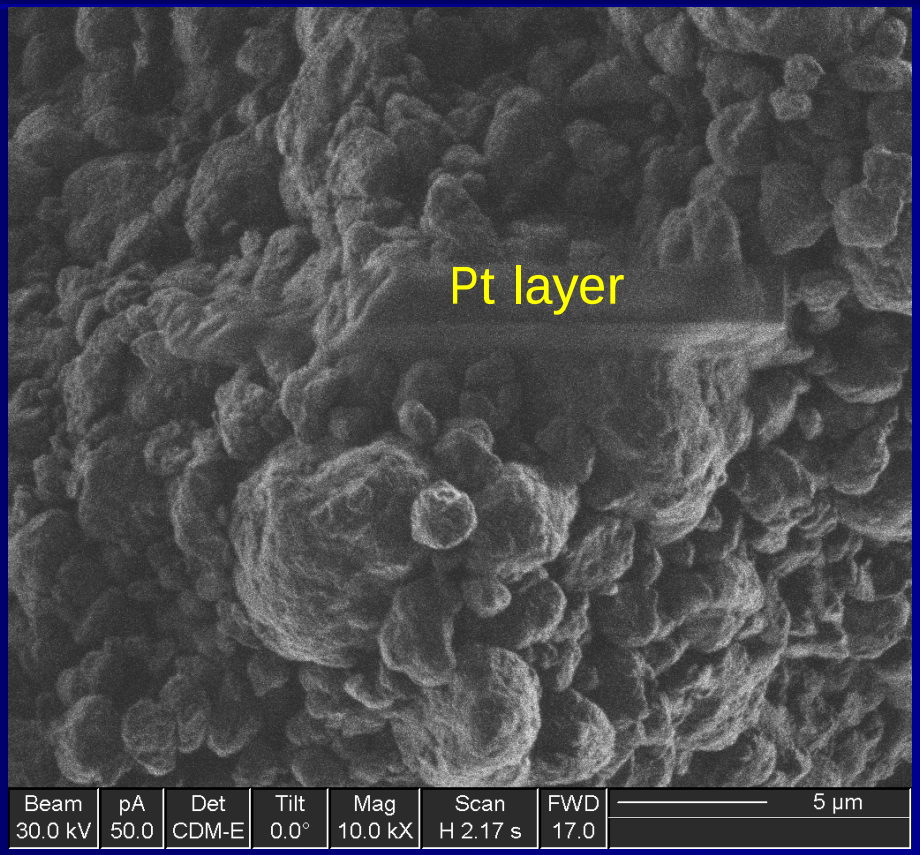

Deposition of a protective Pt layer

Ipus et al, Phil. Mag. 89 (2009) 1415

TEM sample preparation

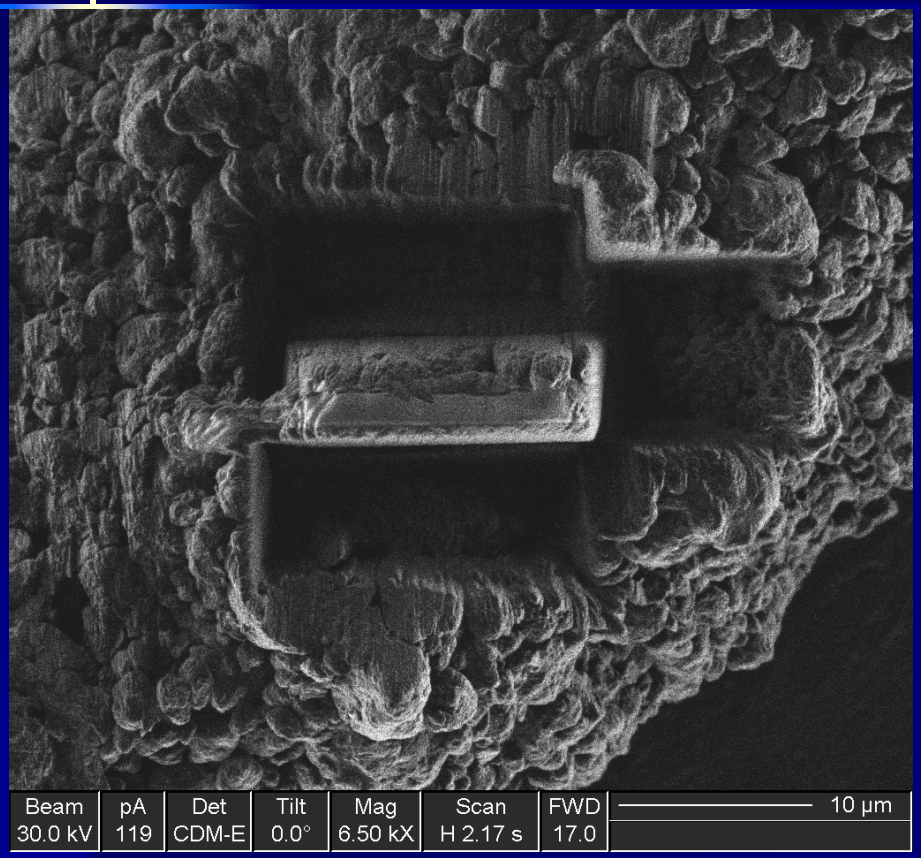

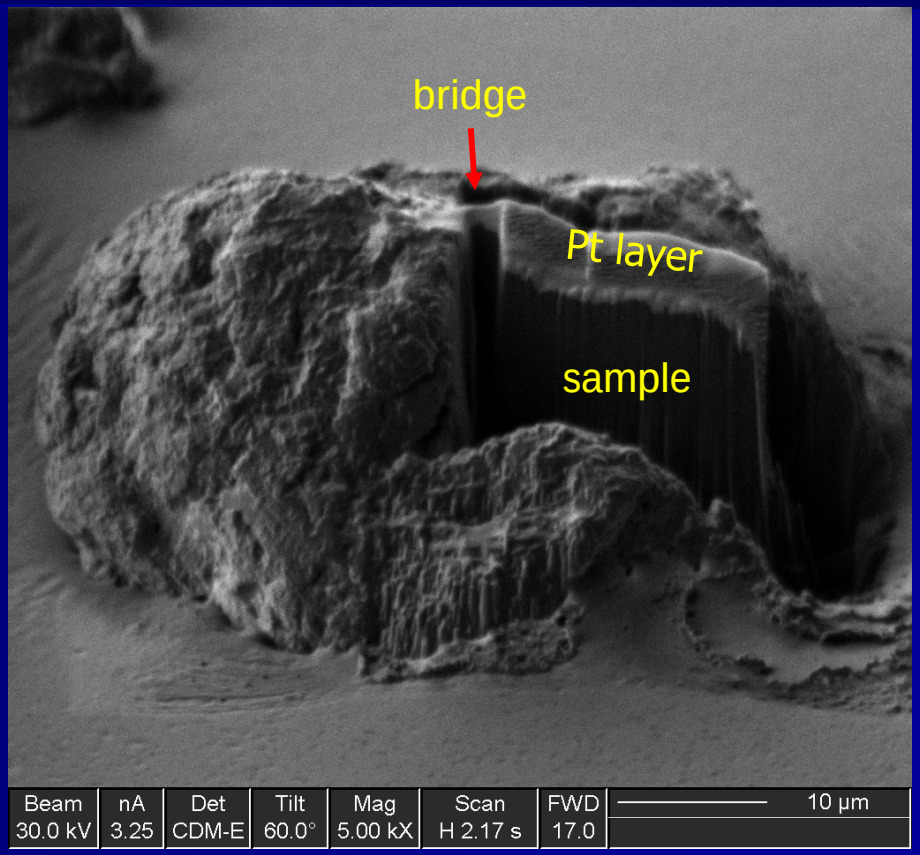

After cutting with Ga ion beam

Ipus et al, Phil. Mag. 89 (2009) 1415

TEM sample preparation

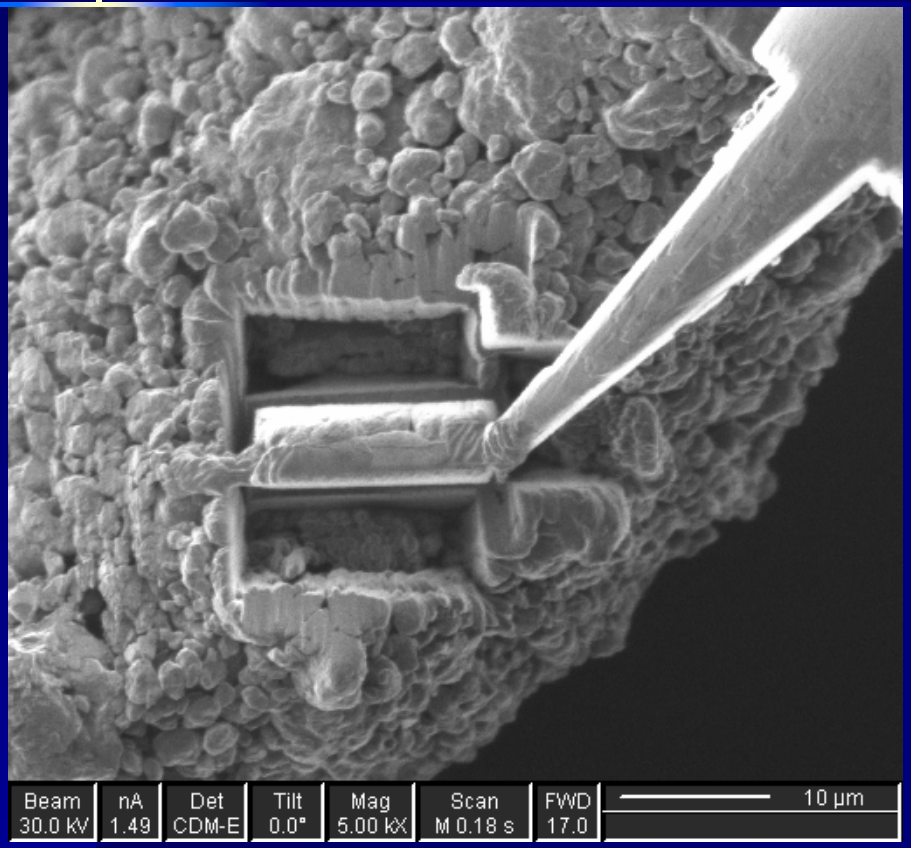

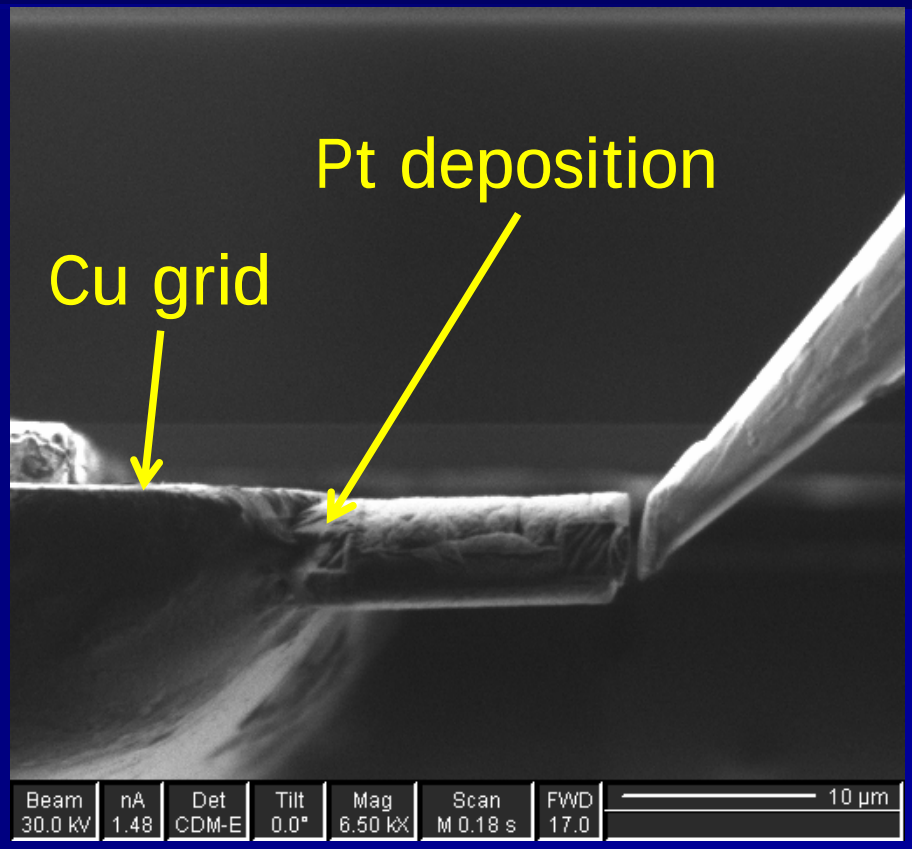

Sample attached to a Cu grid

Ipus et al, Phil. Mag. 89 (2009) 1415

TEM sample preparation

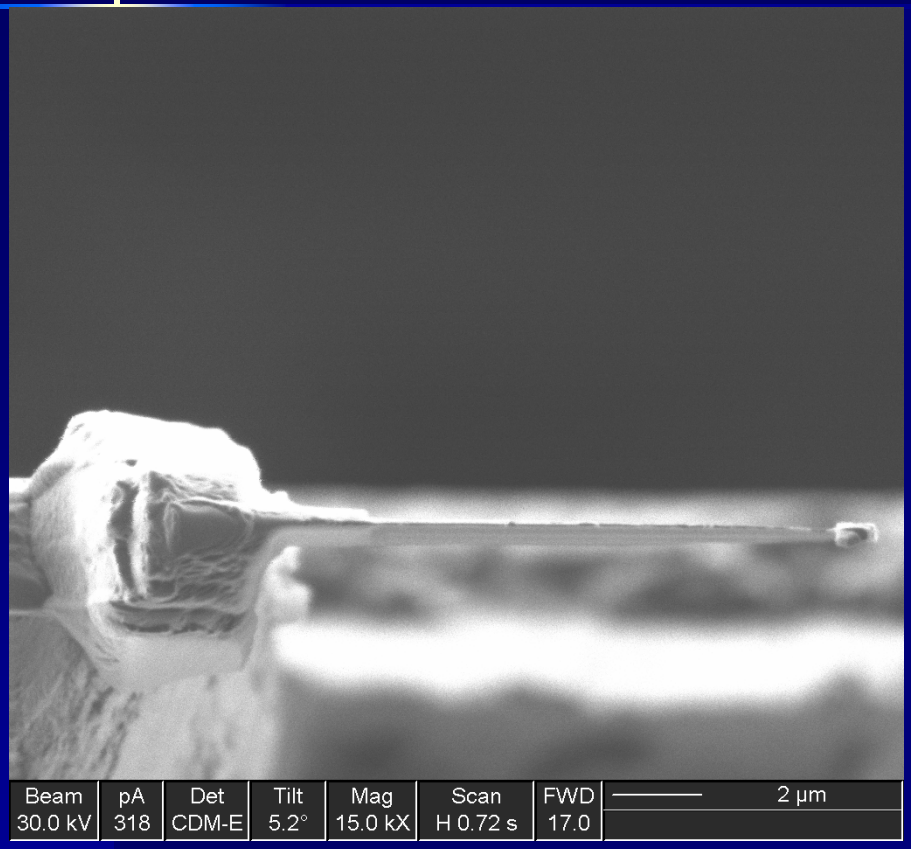

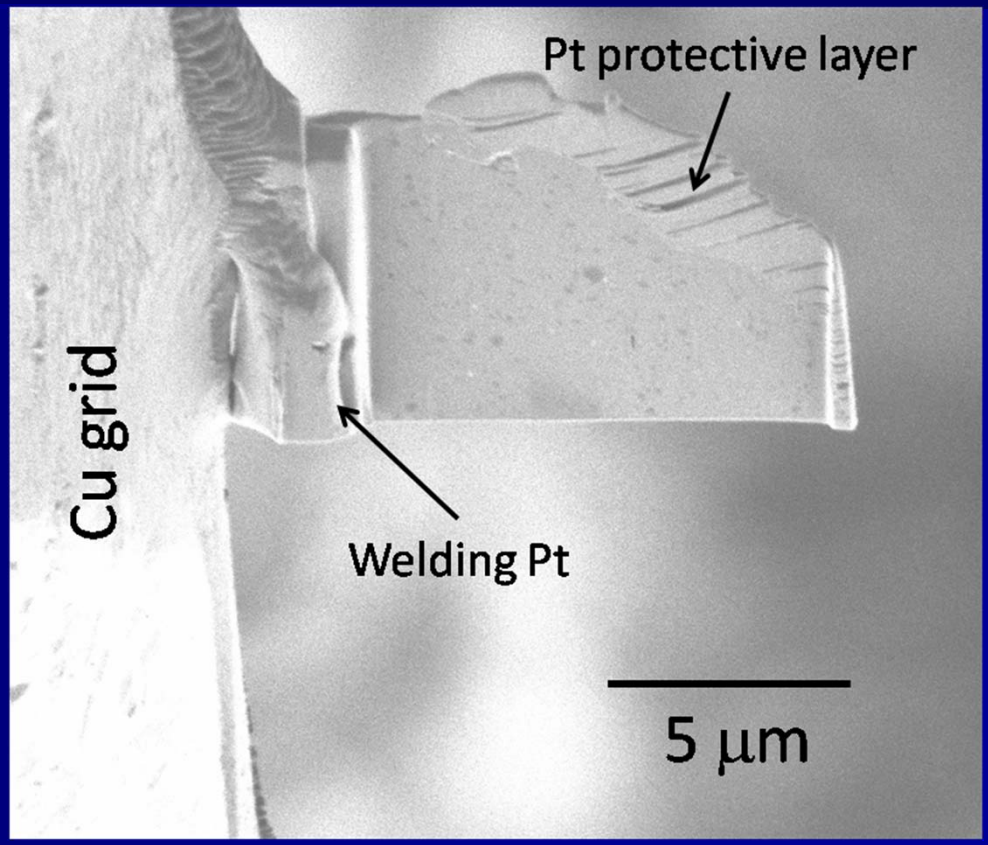

Final thinning using Ga ion beam

Ipus et al, Phil. Mag. 89 (2009) 1415

TEM sample preparation

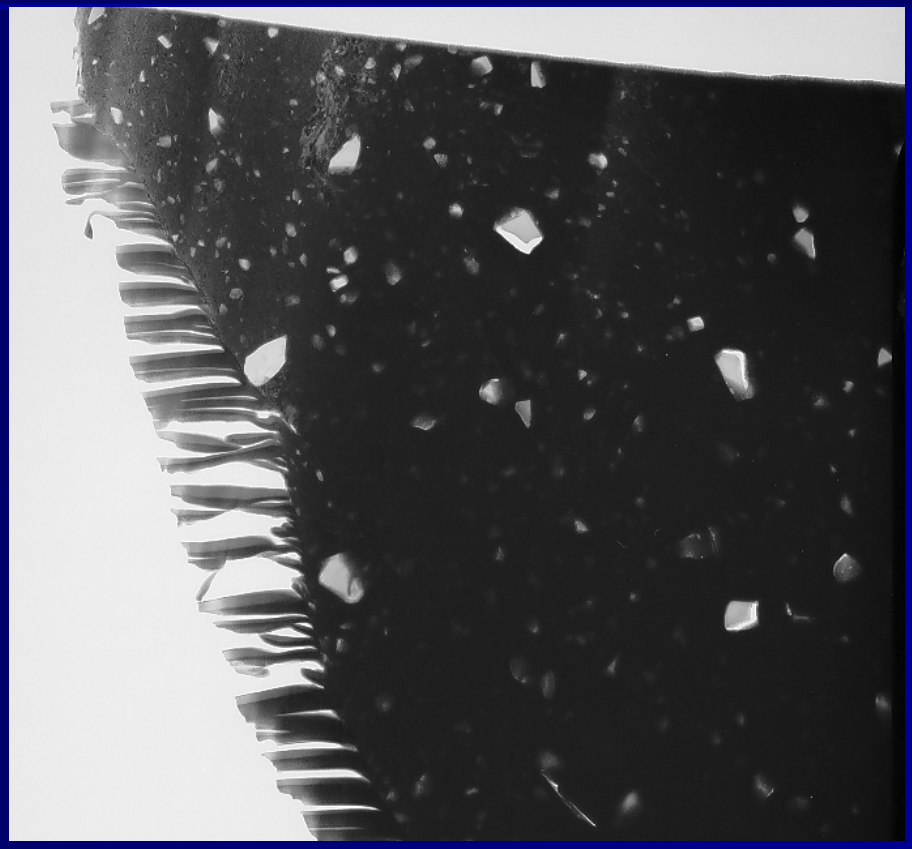

Bright field TEM image of the sample

Ipus et al, Phil. Mag. 89 (2009) 1415

Local microstructure

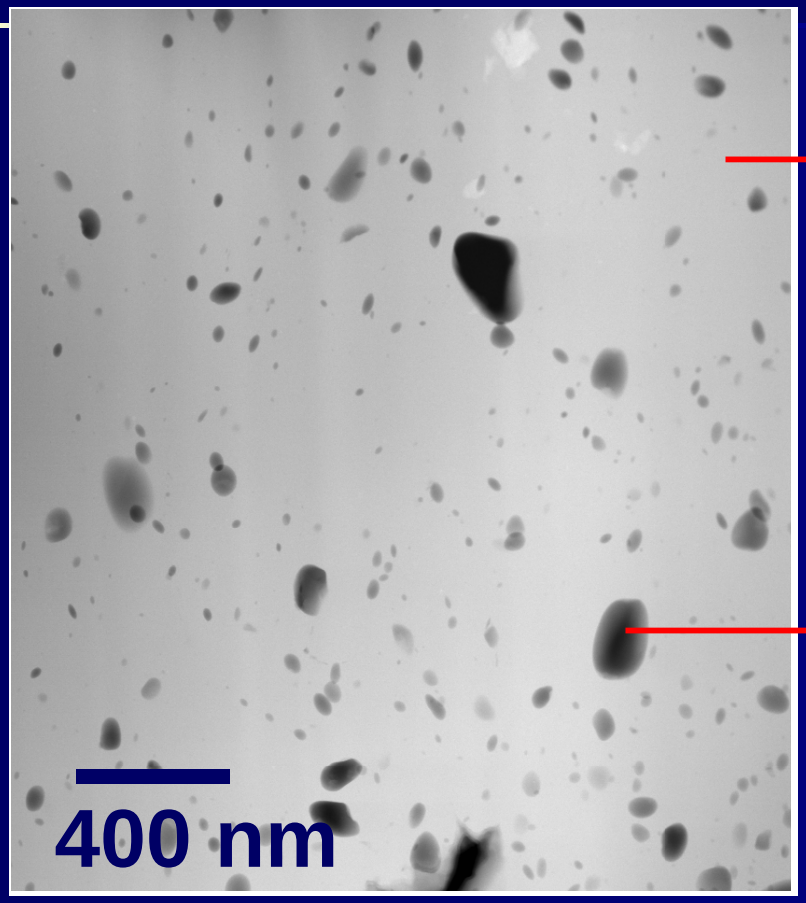

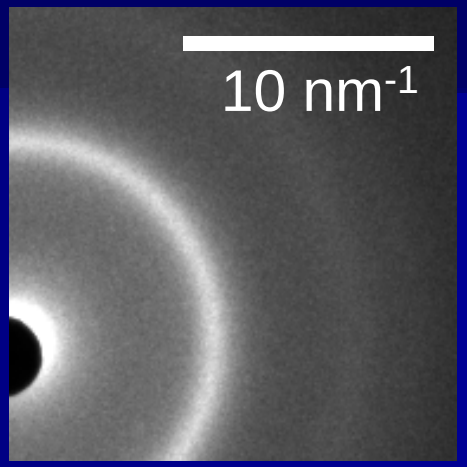

SAD
amorphous
matrix

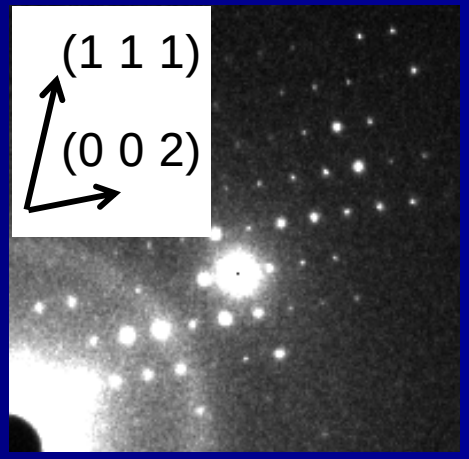

CBED
crystalline
inclusion

Amorphous matrix with boron inclusions and dispersed α-Fe type nanocrystals

Microanalysis

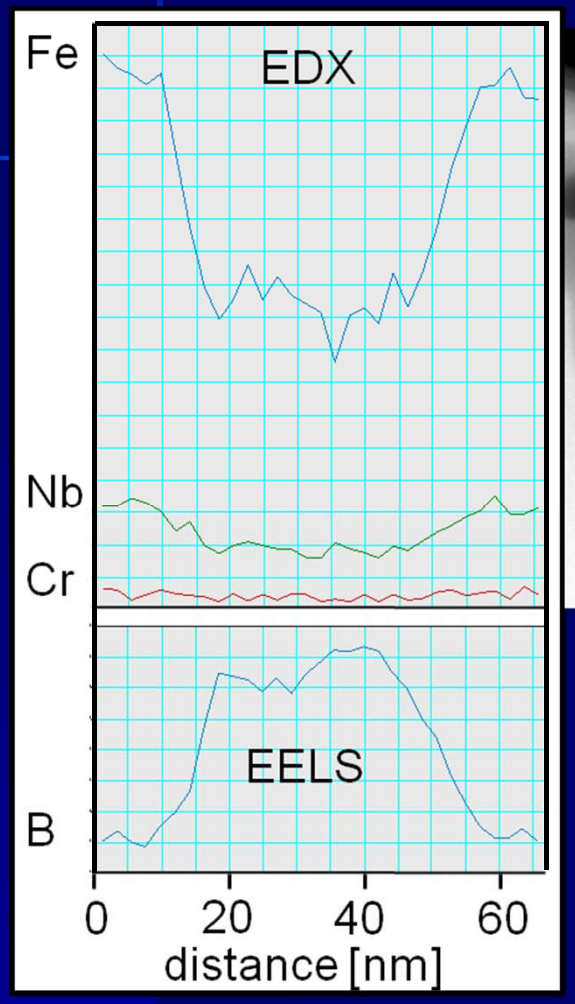

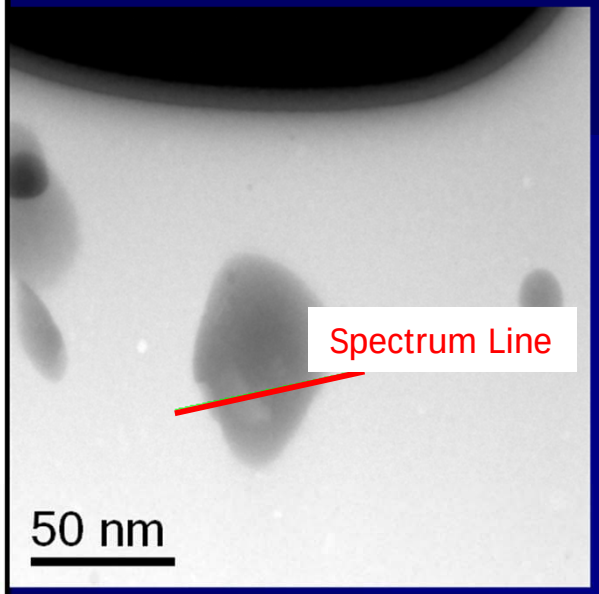

Compositional profiles: line spectra

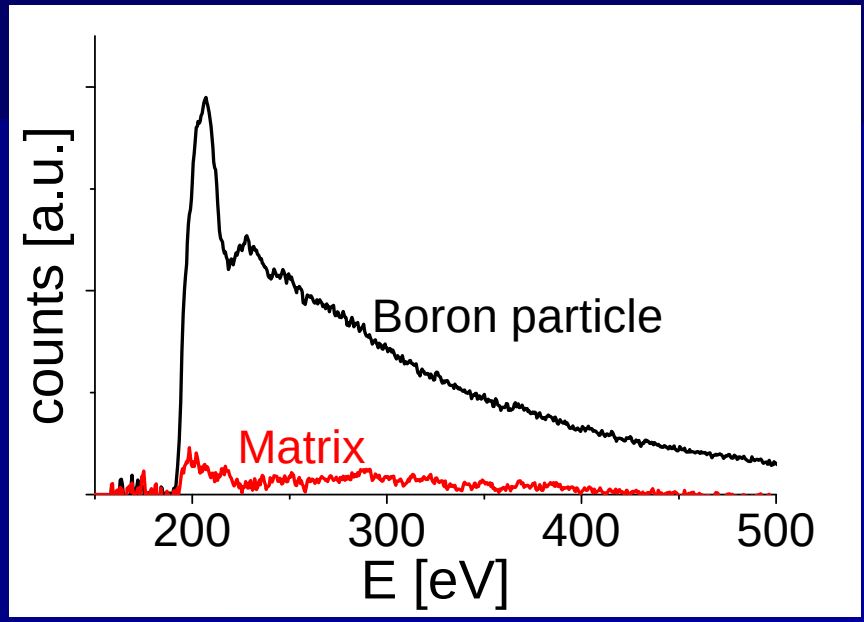

Spot spectra

- Inclusions highly enriched in boron
- Presence of boron in the matrix

Hysteresis loops

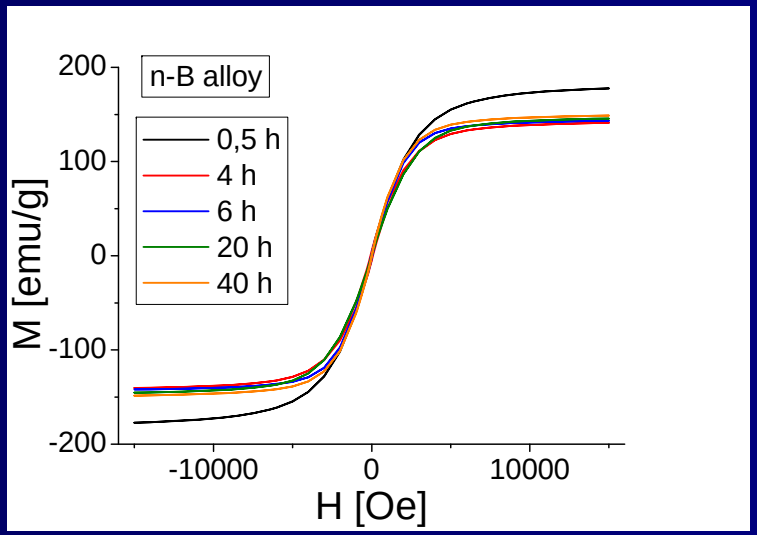

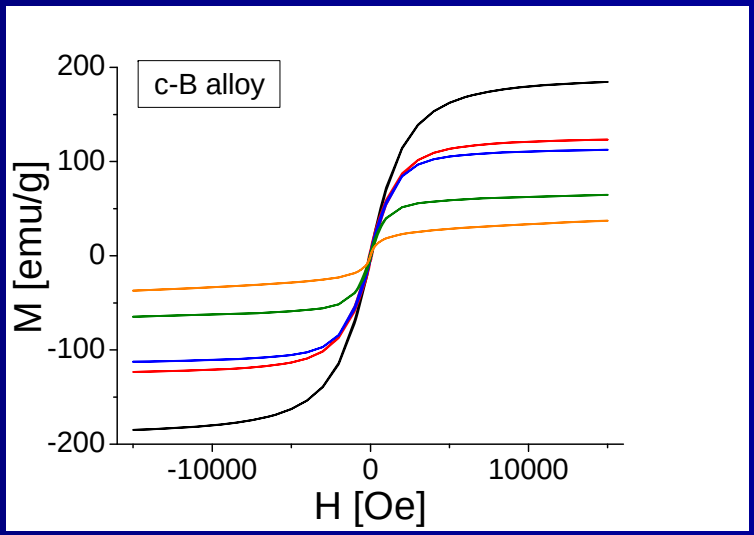

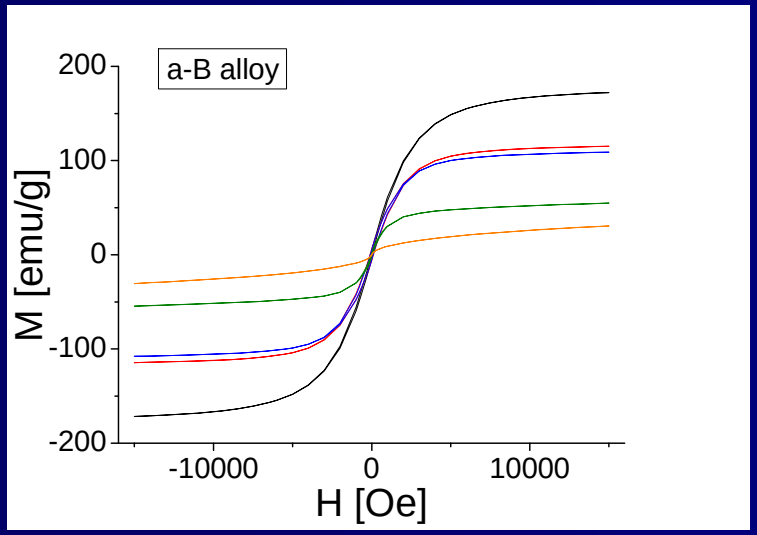

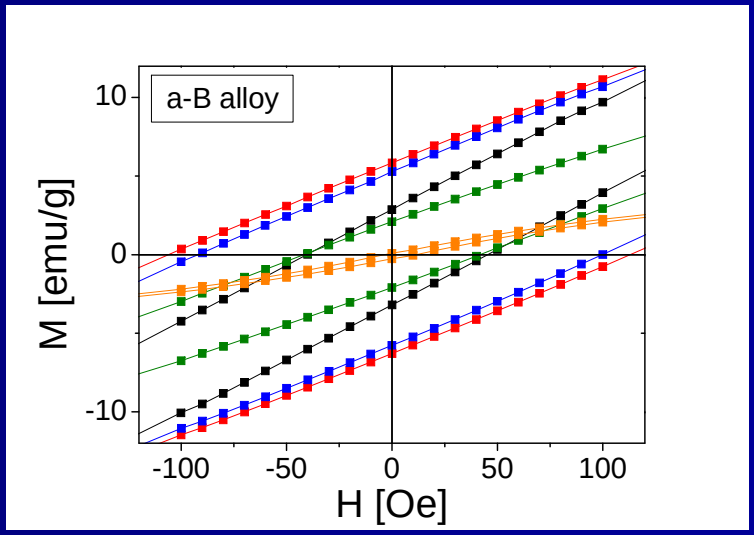

Saturation magnetization

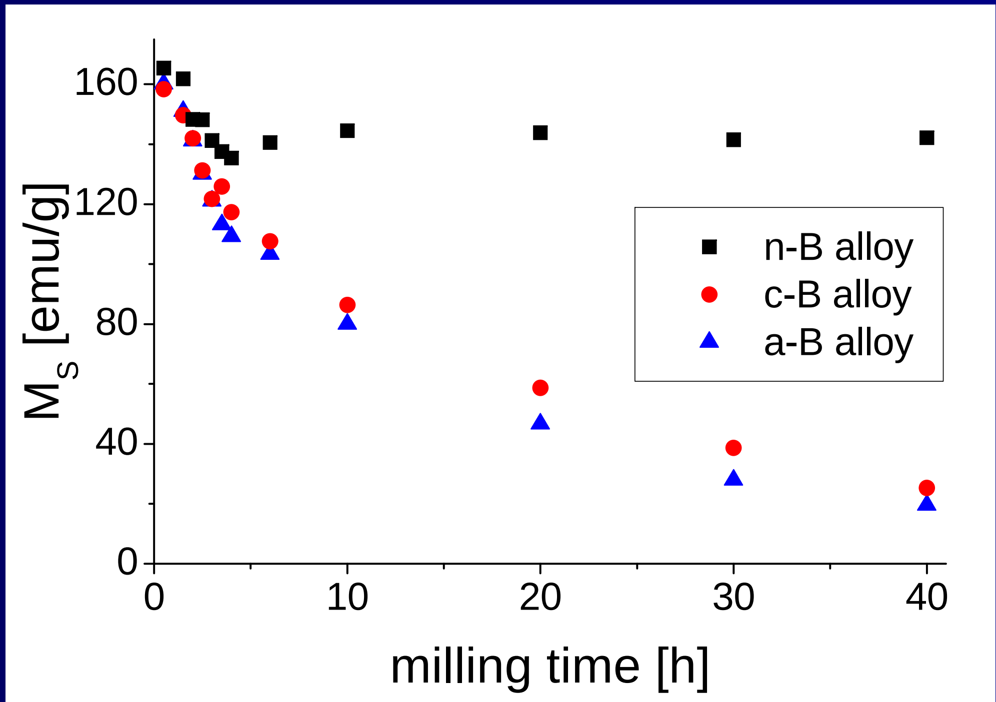

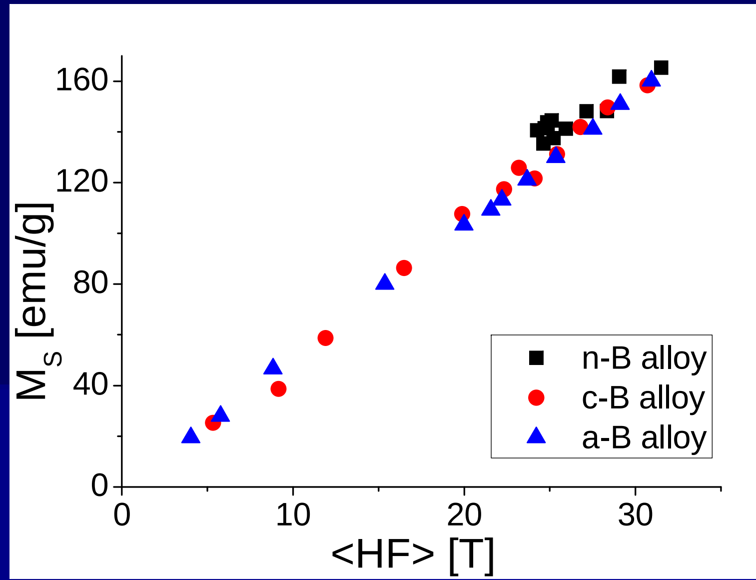

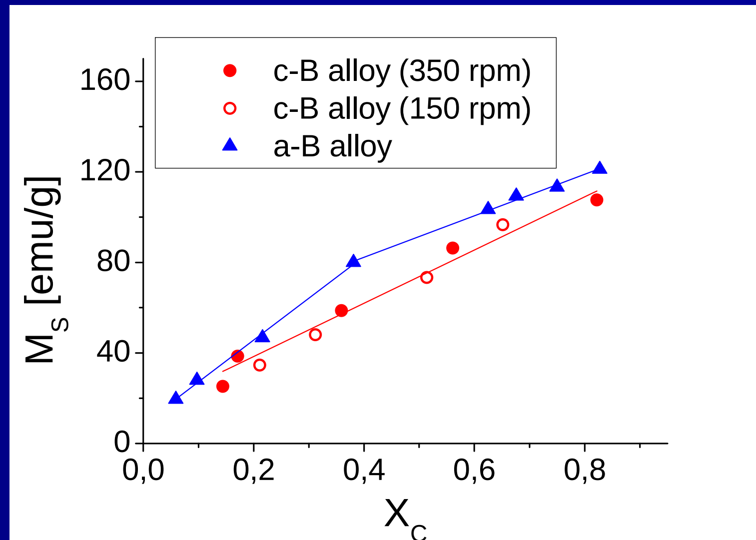

M_S decreases as amorphous phase develops

Different slopes at M_S vs X_C and M_S indicate different rates of B incorporation into the matrix

Coercivity

$$K_{eff} = \frac{M_S \cdot H_C}{p_c}$$

$p_c = 0.64$ for cubic shape particles

Herzer, IEEE Trans Mag 26, 1397 (1990)

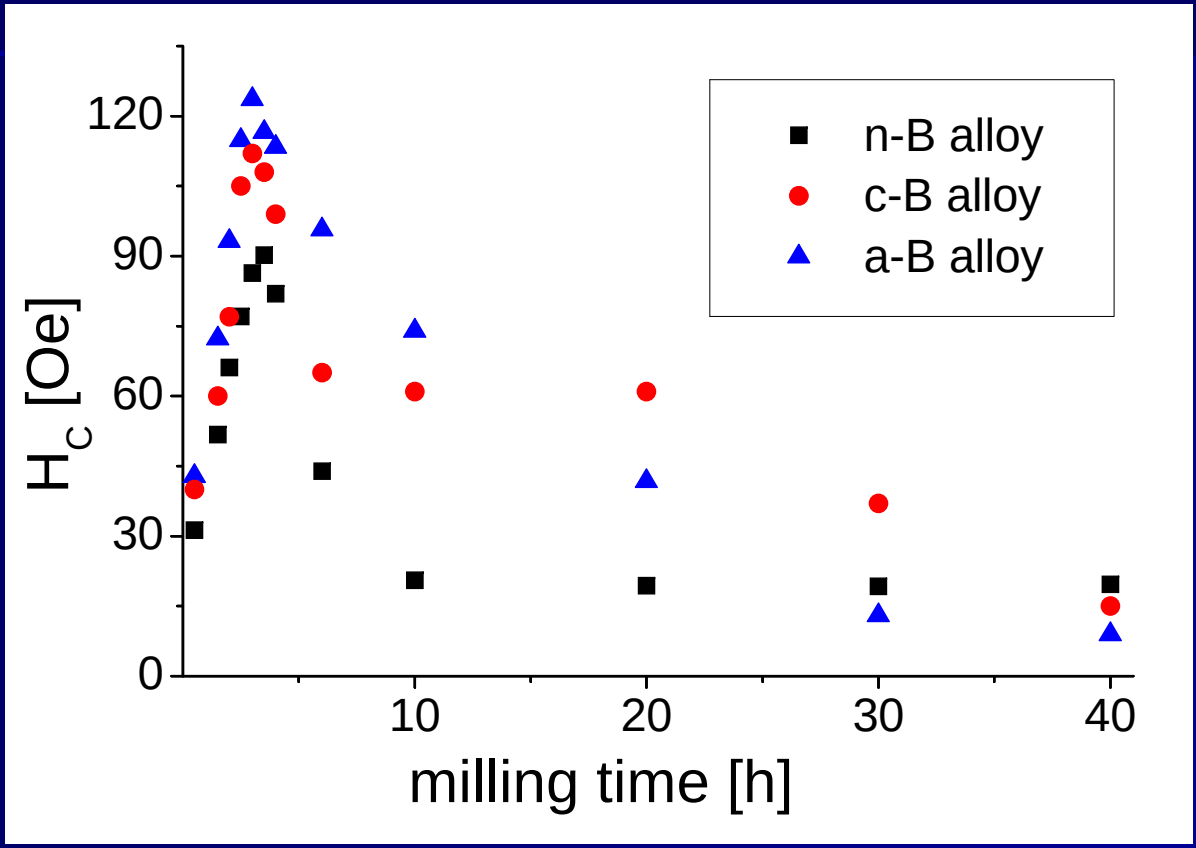

Coercivity initially increases and further on decreases

Magnetic anisotropy

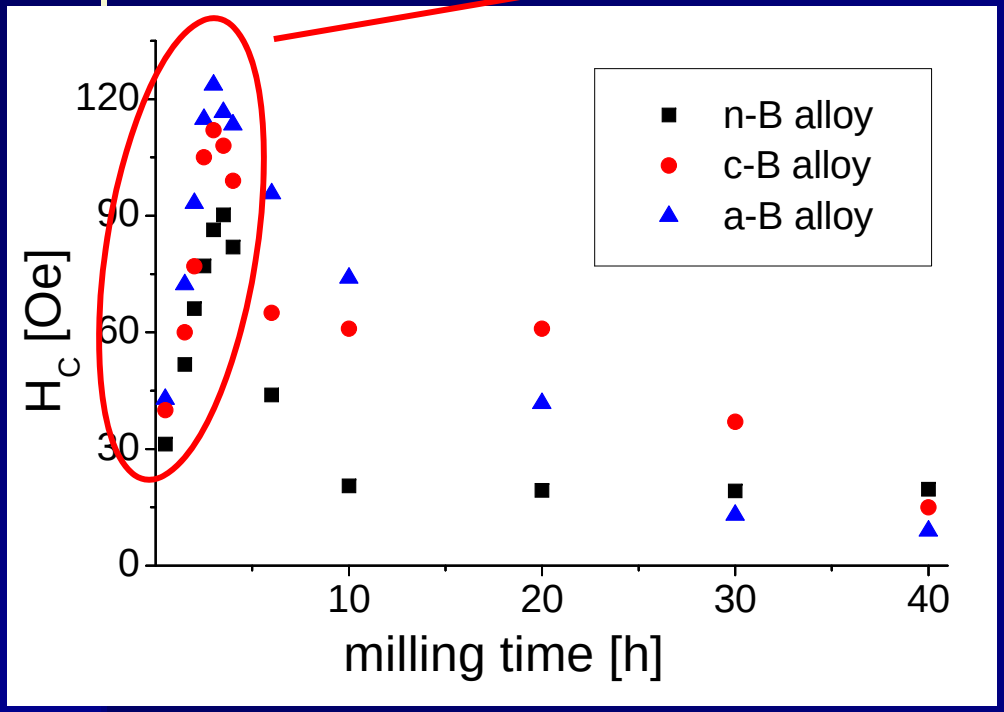

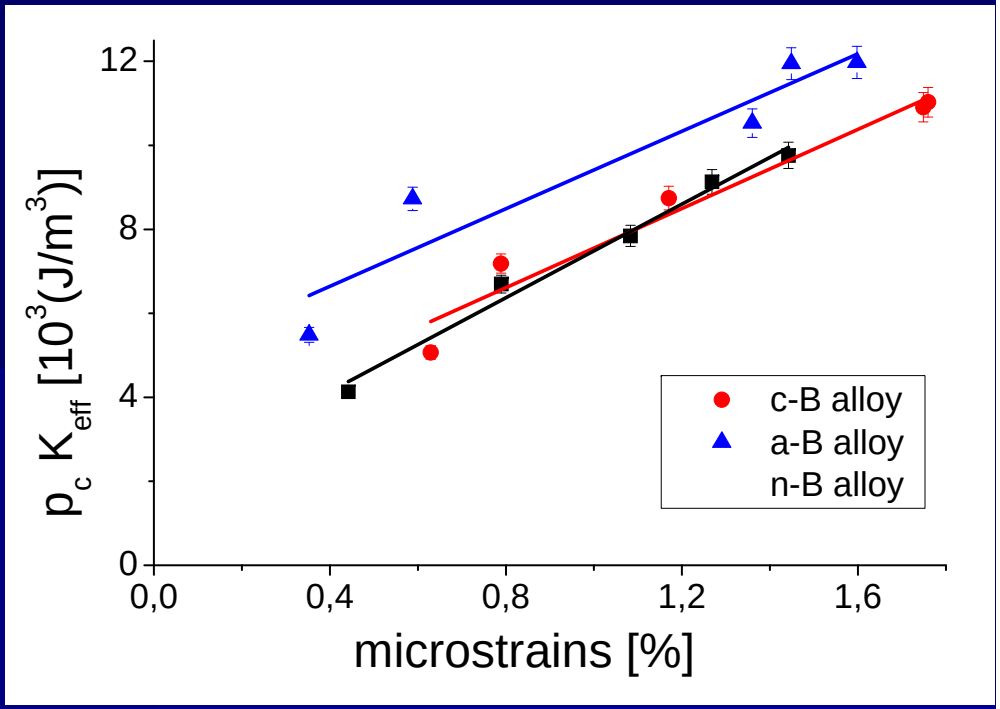

- Initial increase due to the increase of microstrains

Magnetic anisotropy

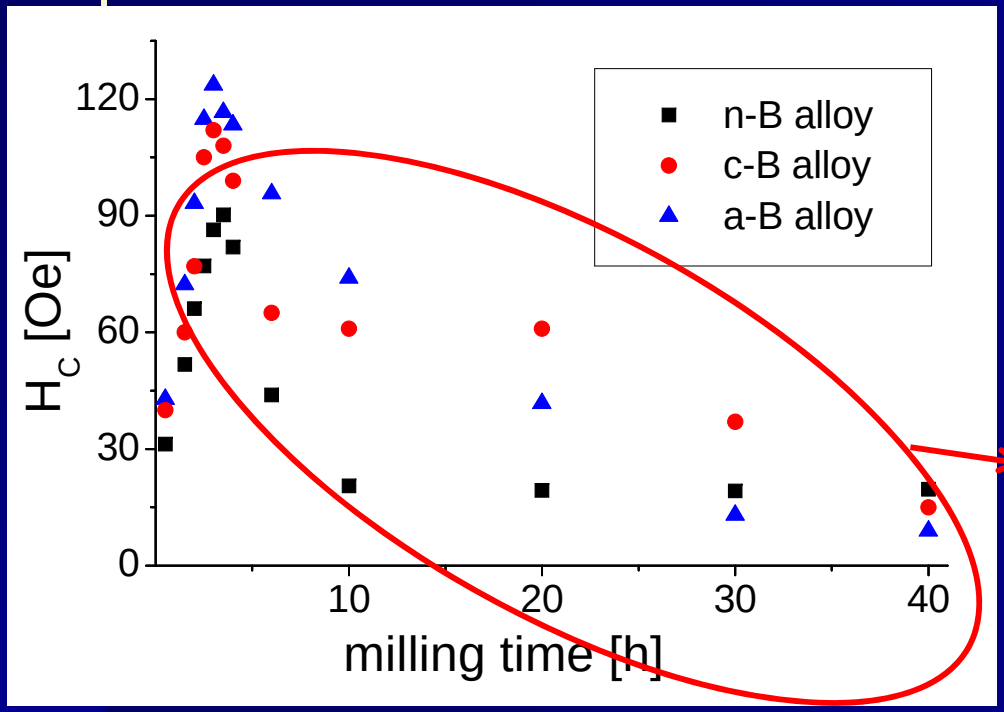

- Reduction after 6h due to crystal refinement

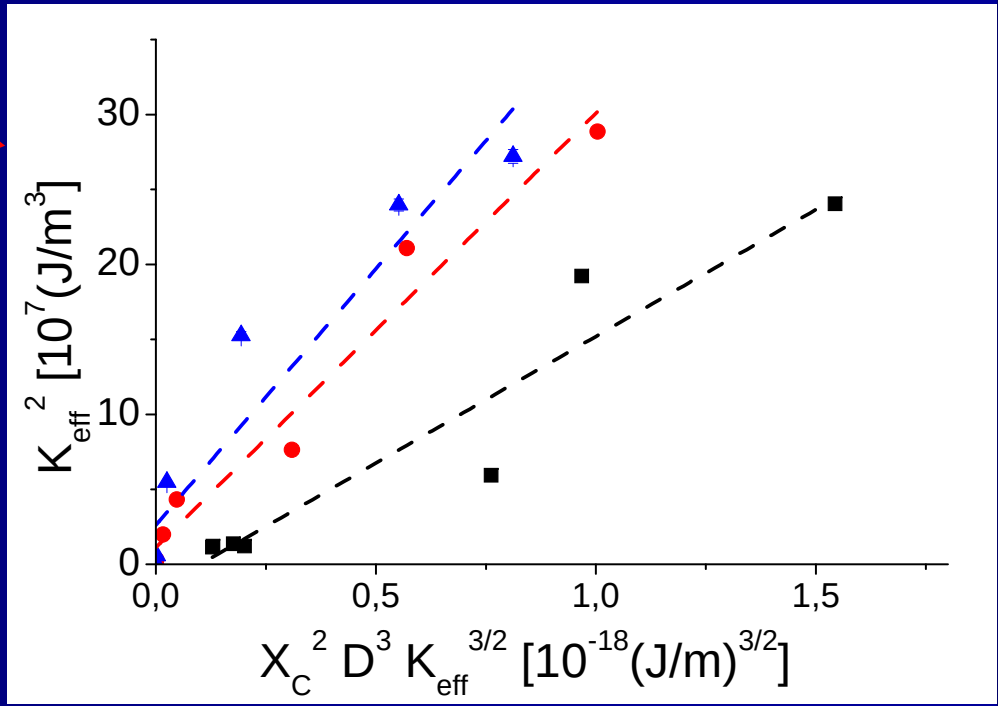

$$K_{eff} = \sqrt{\left(\frac{3}{2}\lambda_S \sigma_{ma}\right)^2 + \left[\left(\frac{3}{2}\lambda_S \sigma_{mi}\right)^2 + K_1^2\right]\frac{X_C^2 D^3 K_{eff}^{3/2}}{A^{3/2}}}$$

Shen, Phys. Rev. B 72, 014431 (2005); Ipus Phys. Express 2, 8 (2012)

LOSSES

Hysteresis losses

- Quasistatic hysteresis loop
- Energy dissipated in a toroidal core over one cycle

$$W = \int_{t=0}^{t=T} i(t)V(t)dt$$

- Combining Ampere and Lenz laws

$$W = lA\int_{t=0}^{t=T} H\frac{dB}{dt}dt = lA\oint HdB$$

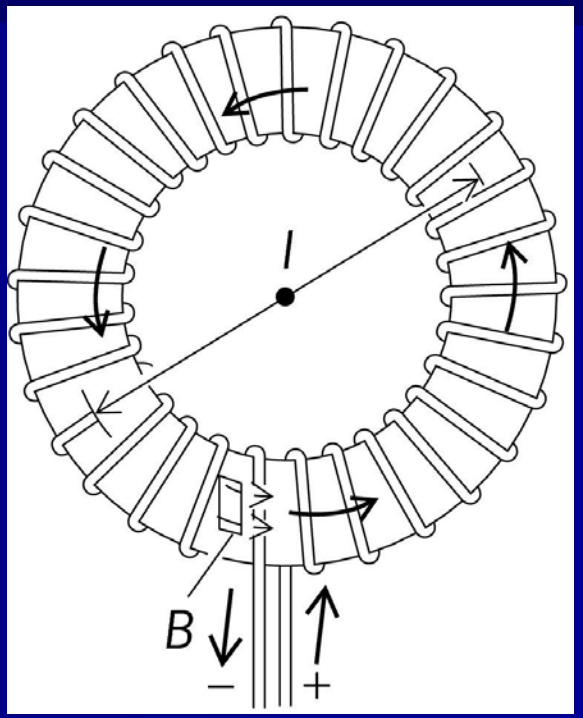

- The energy lost per unit volume is given by the area of the loop

Increasing frequency

- Loops get broader and rounder
- Effect of eddy currents induced in the material
- Change in M→induced voltage which opposes the flux change
- Losses emerge due to the heating of the sample due to these currents

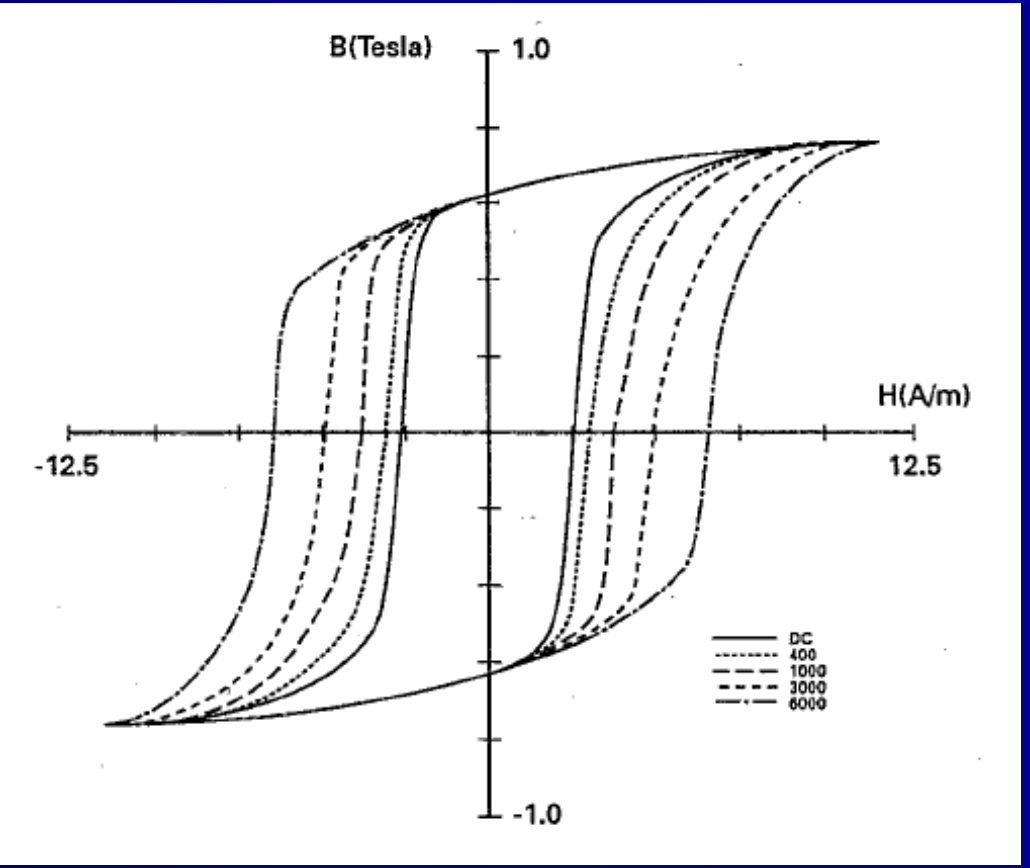

D.C. Jiles, J. Appl. Phys. 76 (1994) 5849

Classical eddy currents

- The material is uniformly magnetized
- Change in M→induced voltage which opposes the flux change
- Losses emerge due to the heating of the sample caused by these currents i^2R
- Powe loss per unit volume at low frequency

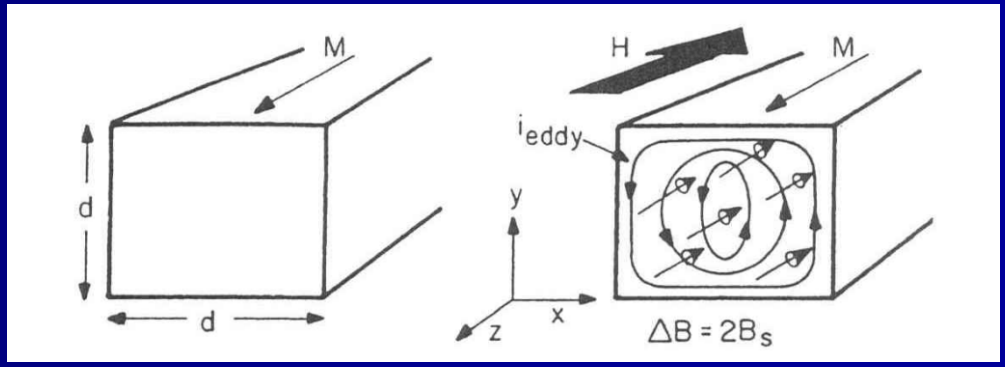

R.C. O'Handley, "Modern Magnetic Materials", Willey, 2000

- Reduce losses by:
  - Reduzing d
  - Increasing resistance

$$P_{class} / vol \propto \frac{\omega^2 B_m^2 d^2}{\rho}$$

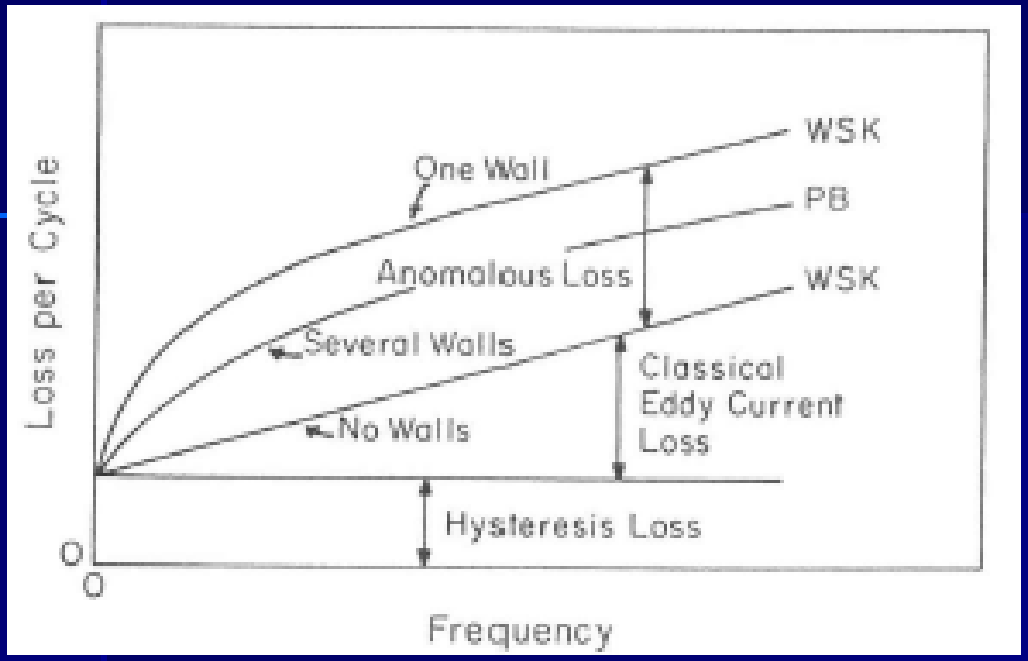

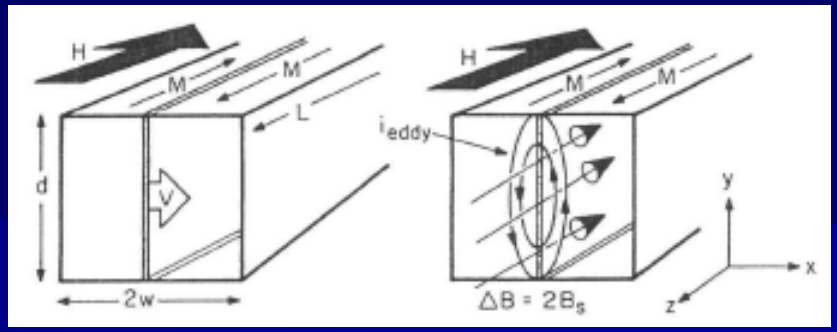

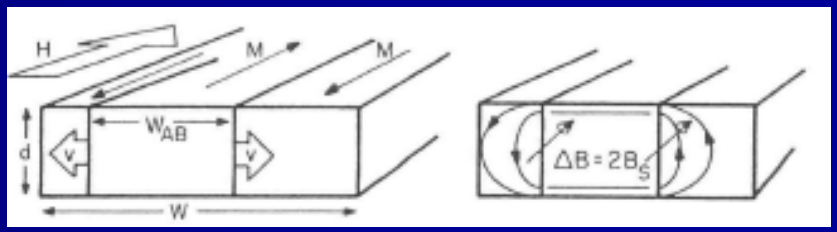

- The flux change is restricted to the environment of the wall
- Losses depend on the velocity of the wall
  - Drag field
- For multiple walls, currents interfere and reduce the losses

Influence of induced anisotropies

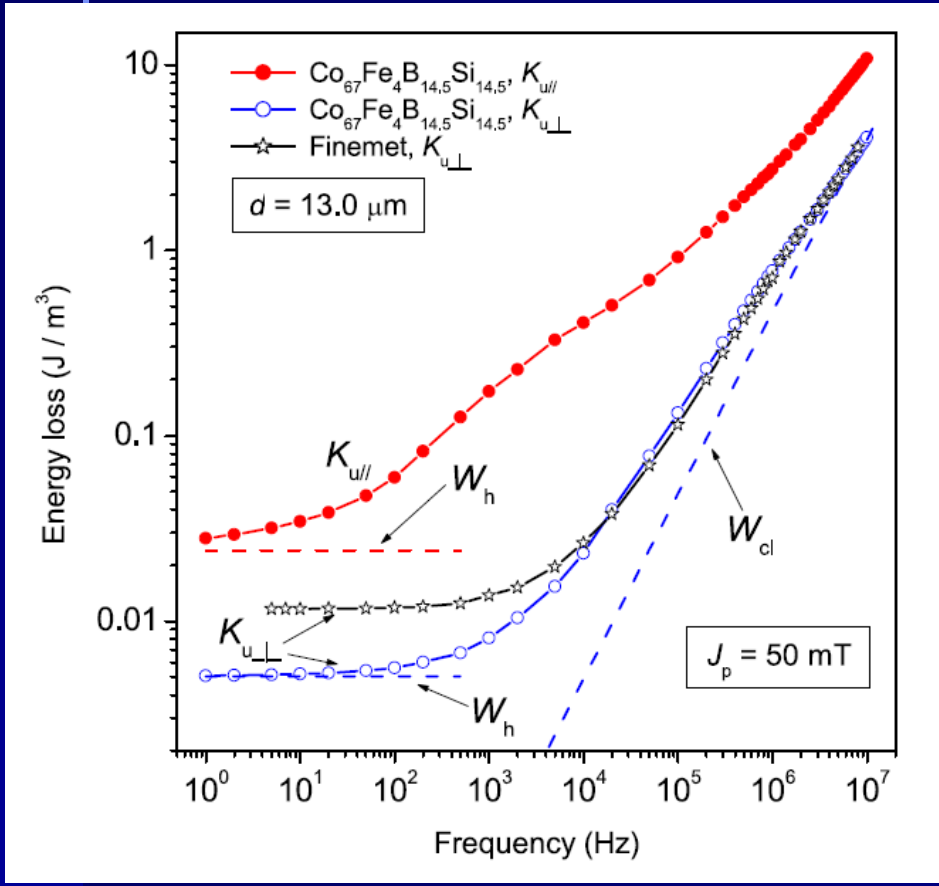

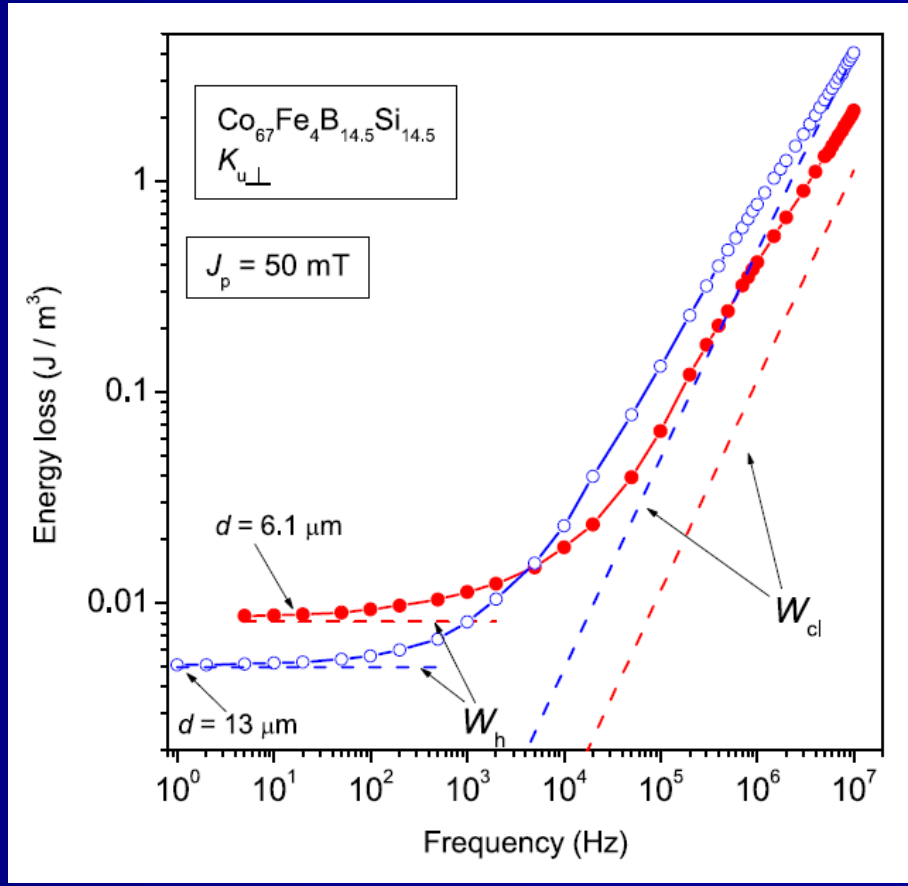

F. Fiorillo, C. Beatrice, J Supercond Nov Magn 24 (2011) 559

More sofisticated models

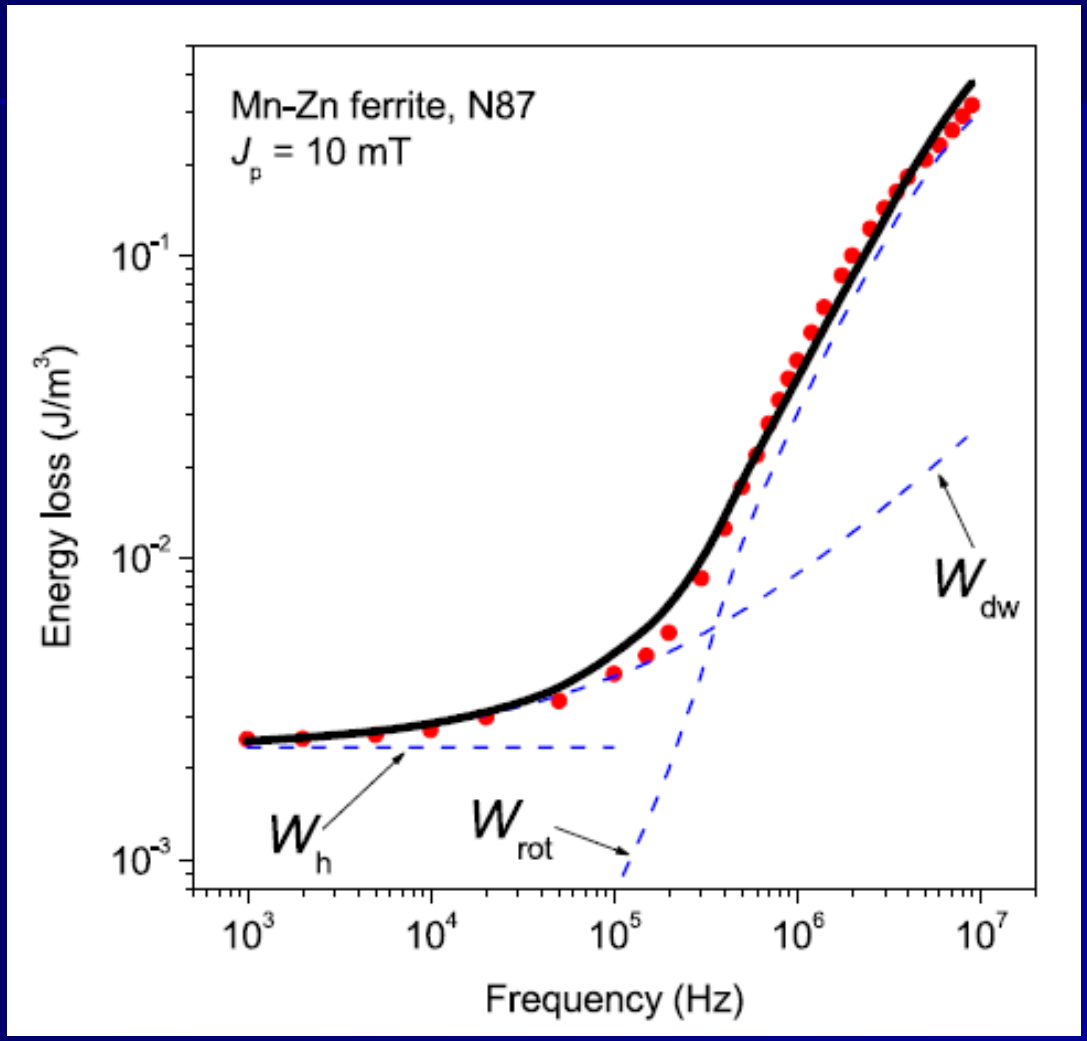

F. Fiorillo, C. Beatrice, J Supercond Nov Magn 24 (2011) 559

Perspectives of core loss reduction in GOSS

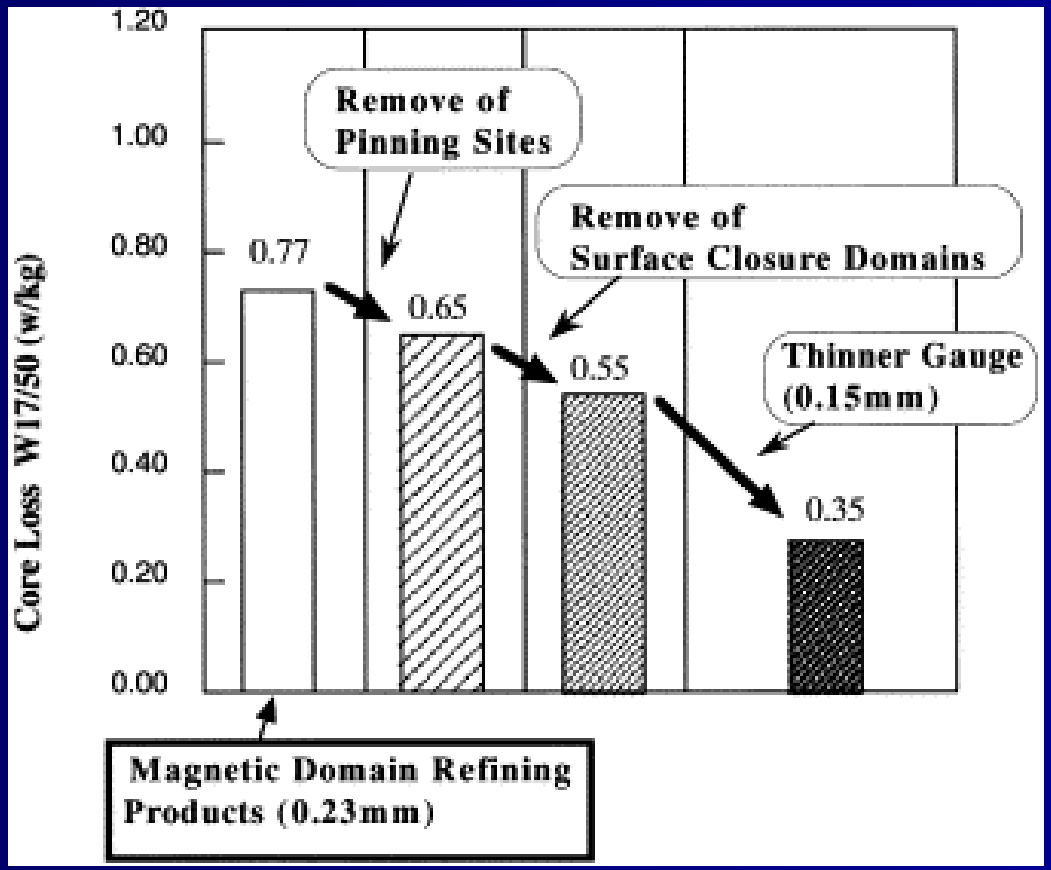

T. Kubota, M. Fujikura, Y. Ushigami J. Magn. Magn. Mater. 215-216 (2000) 69

HIGH FREQUENCY POWER CONVERSION

- Designing an inductive component

$$V = -NA\frac{dB}{dt} = -L\frac{dI}{dt} = -LI_o\omega\cos(\omega t) = \frac{-\mu N^2 A}{l} I_o\omega\cos(\omega t)$$

- For the same voltage amplitude, the section is inversely proportional to the frequency
- Go to higher frequencies in power converters to decrease the volume and weight

- High frequency power converters use active switching circuits and PWM
  - Superposition of many frequencies
  - Materials should have broadband capabilities
- Heat dissipation in the inductors
  - Scaling down the surface while keeping the dissipated heat brings thermal management problems
- We have to add winding losses and core losses

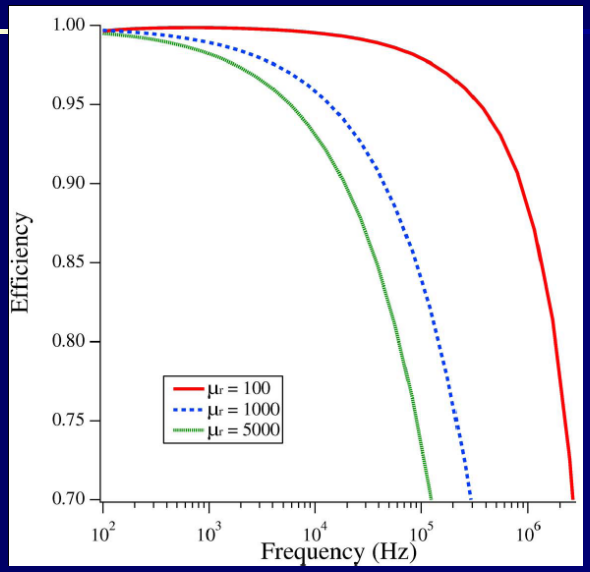

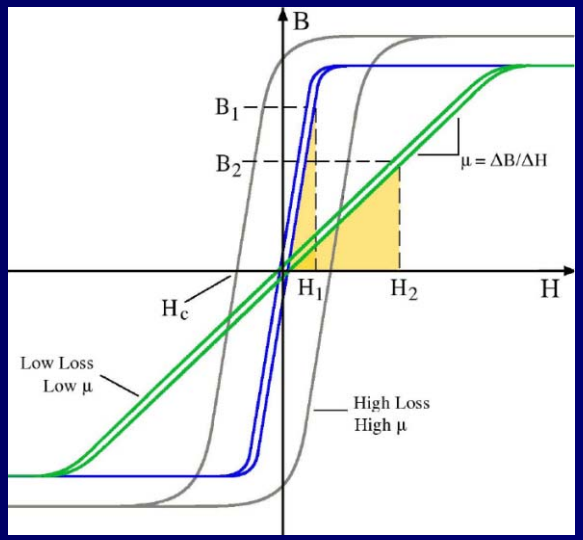

- Lower permeability allows larger efficiency under some circumstances
- For the same induction, we need larger H (more current or more turns) for lower permeability materials
- Depending if the added stored energy is larger than the additional heating, it could be beneficial

A.M. Leary, P.R. Ohodnicki, M.E. McHenry, JOM 64 (2012) 772

SENSORS:
GIANT MAGNETO IMPEDANCE

The (very) basics of GMI

- Skin penetration depth $\delta \propto \sqrt{\frac{\rho}{\omega\mu}}$

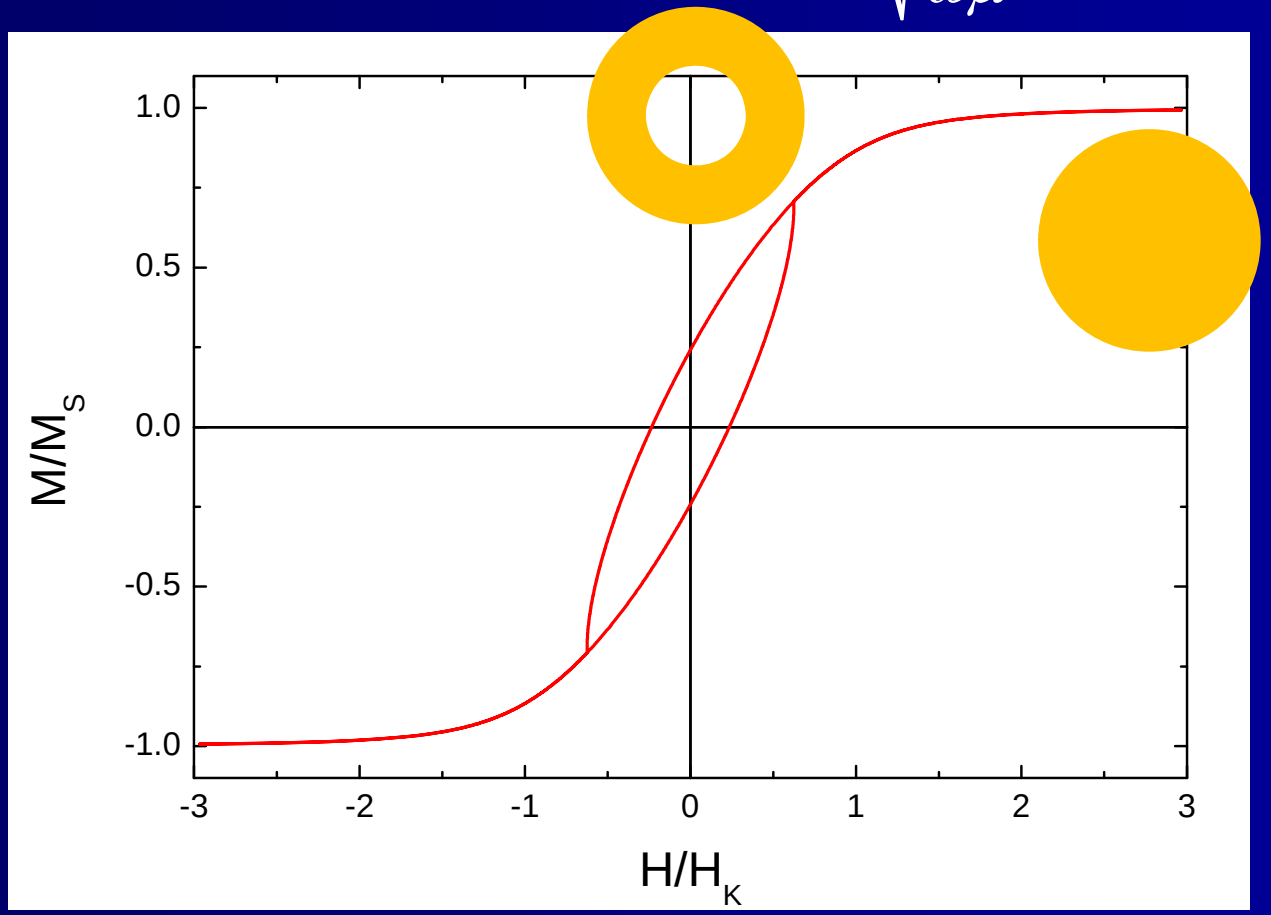

Giant magnetoimpedance

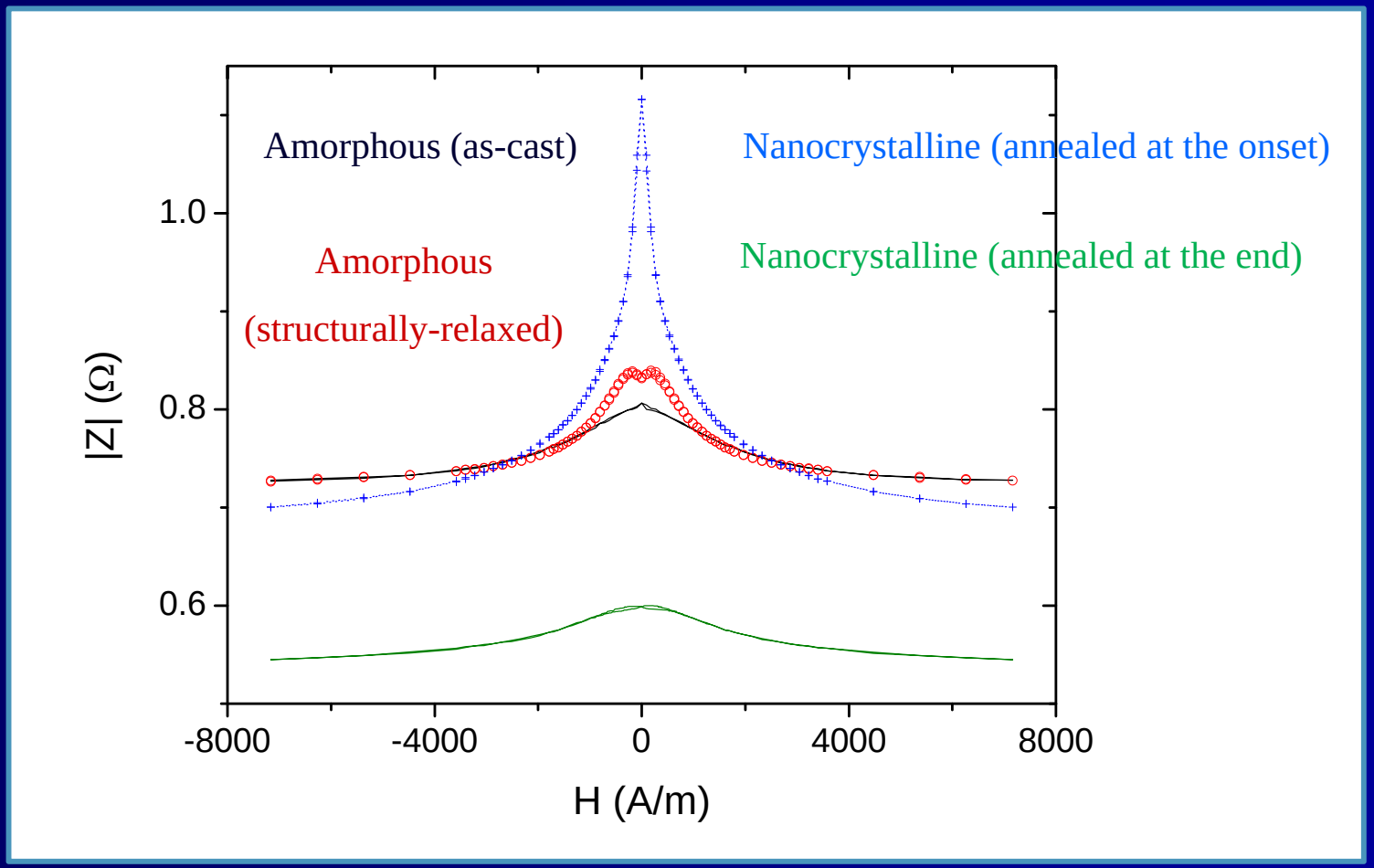

GMI vs Fluxgate field sensors

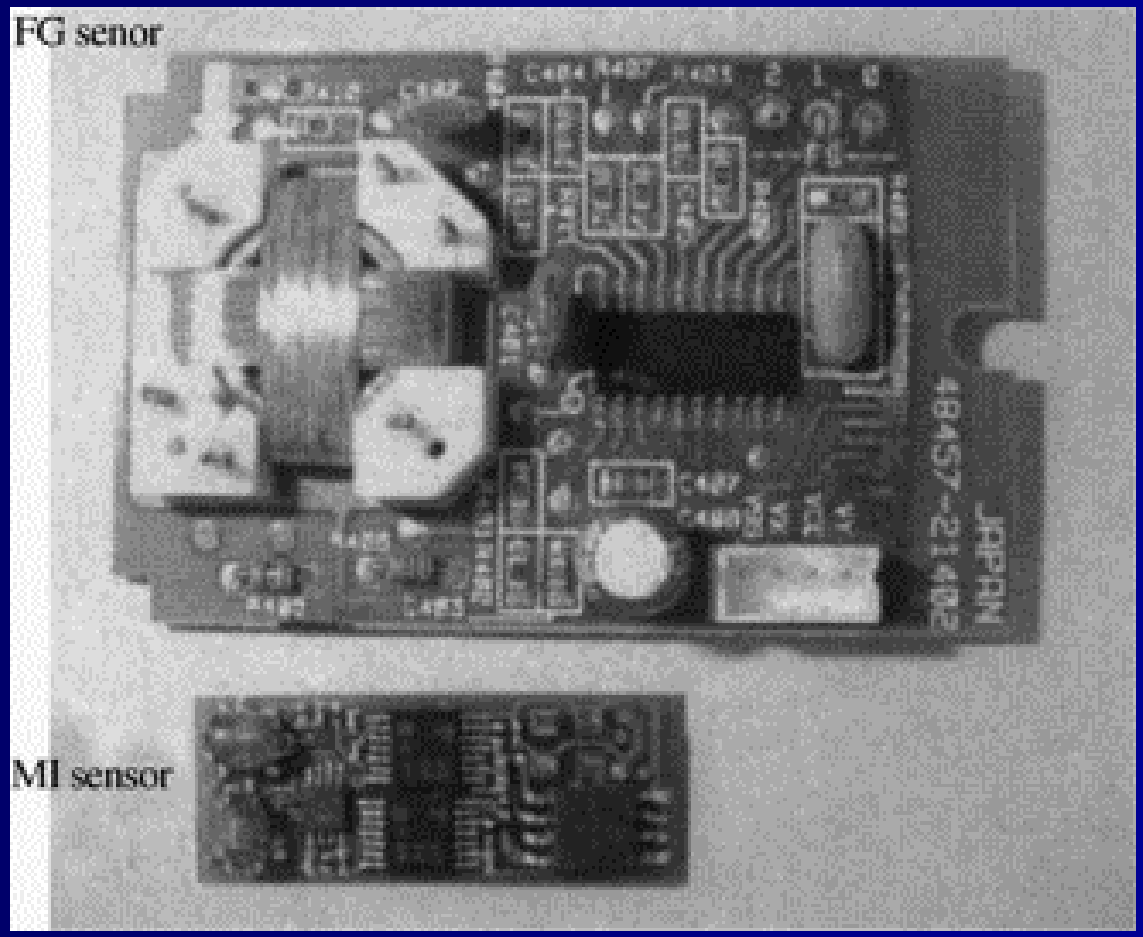

Y. Honkura, J Magn Magn Mater 249 (2002) 375

Relationship anisotropy/GMI

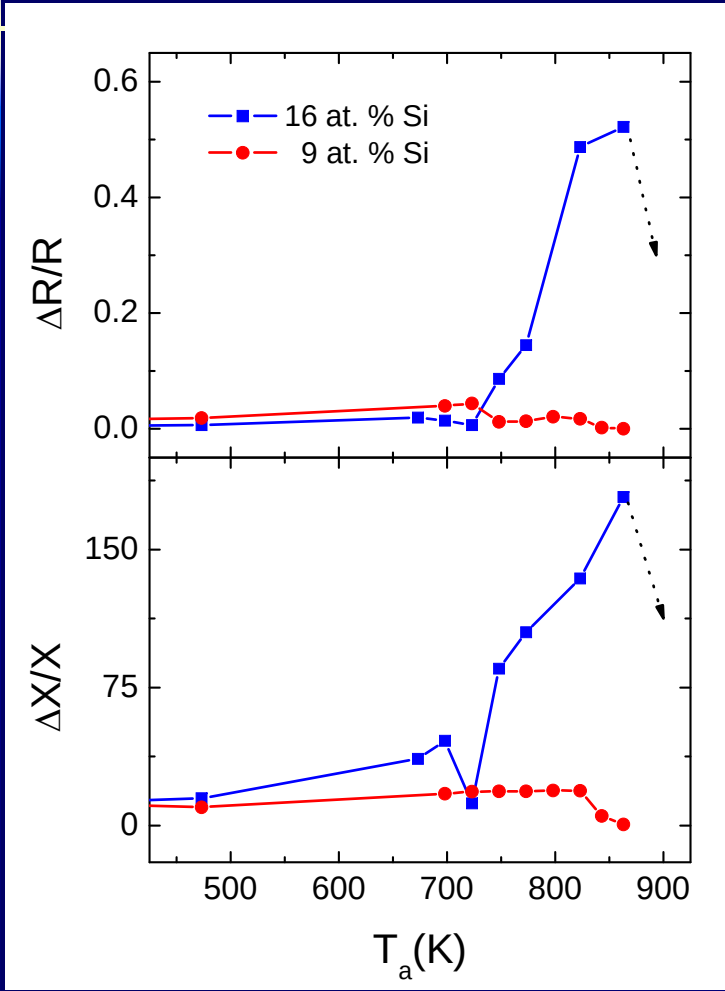

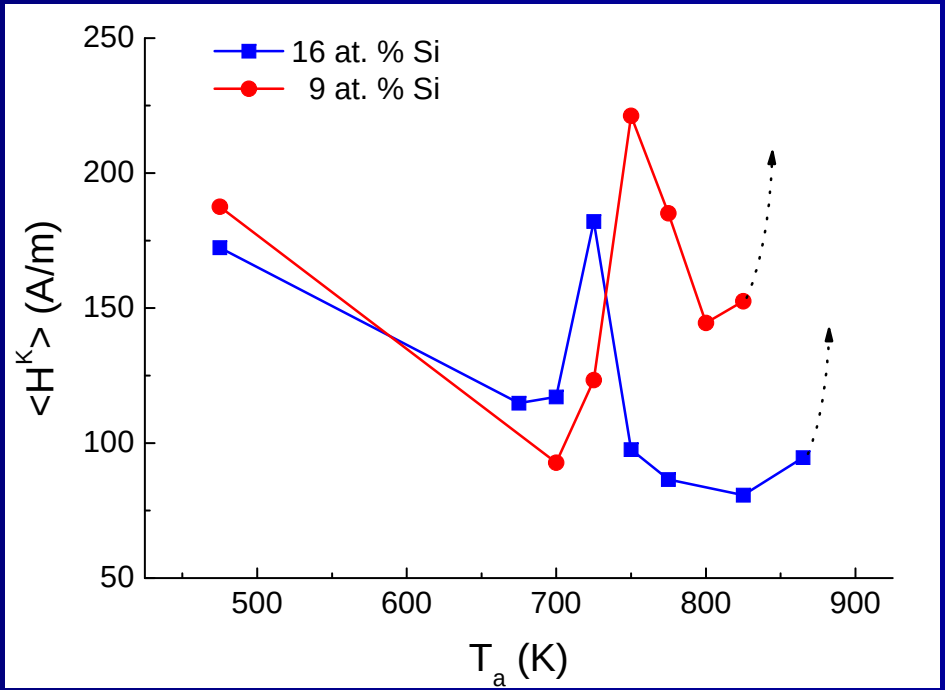

V. Franco, A. Conde, Materials Letters 49 (2001) 256

Conclusions

- Soft magnetic materials are used in numerous energy-related applications
- Coercivity can be optimized by properly designing the microstructure of the materials
  - Random anisotropy model
- High temperature soft magnetic amorphous alloys are a challenge
- Amorphous and nanocrystalline alloys can be a good testing ground to develop models of multiphase magnetic systems